Soil nitrous oxide emissions across the northern high latitudes

Naiqing Pan[1], Hanqin Tian[2], Hao Shi[3], Shufen Pan[4], Josep G. Canadell[5], Jinfeng Chang[6], Philippe Ciais[7], Eric A. Davidson[8], Gustaf Hugelius[9], Akihiko Ito[10], Robert B. Jackson[11], Fortunat Joos[12], Sebastian Lienert[13], Dylan B. Millet[14], Stefan Olin[15], Prabir K. Patra[16], Rona L. Thompson[17], Nicolas Vuichard[18], Kelley C. Wells[14], Chris Wilson[19], Yongfa You[20], and Sönke Zaehle[21]

[1]Boston College
[2]Schiller Institute for Integrated Science and Society, Boston College
[3]Research Center for Eco-Environmental Sciences
[4]Auburn University
[5]Global Carbon Project, CSIRO Oceans and Atmosphere
[6]Zhejiang University
[7]Laboratory for Climate Sciences and the Environment (LSCE)
[8]University of Maryland Center for Environmental Science
[9]Stockholm University
[10]National Institute for Environmental Studies
[11]Stanford University
[12]University of Bern
[13]Climate and Environmental Physics, Physics Institute and Oeschger Centre for Climate Change Research, University of Bern
[14]University of Minnesota
[15]Lund University
[16]JAMSTEC
[17]Norwegian Institute for Air Research
[18]LSCE-IPSL
[19]Leeds University
[20]Unknown
[21]Max Planck Institute for Biogeochemistry

April 16, 2024

Abstract

Nitrous oxide (N2O) is the most important stratospheric ozone-depleting agent based on current emissions and the third largest contributor to increased net radiative forcing. Increases in atmospheric N2O have been attributed primarily to enhanced soil N2O emissions. Critically, contributions from soils in the Northern High Latitudes (NHL, >50°N) remain poorly quantified despite their vulnerability to permafrost thawing induced by climate change. An ensemble of six terrestrial biosphere models suggests NHL soil N2O emissions doubled since the preindustrial 1860s, increasing on average by 2.0±1.0 Gg N yr-1 (p<0.01). This trend reversed after the 1980s because of reduced nitrogen fertilizer application in non-permafrost regions and increased plant growth due to CO2 fertilization suppressed emissions. However, permafrost soil N2O emissions continued increasing attributable to climate warming; the interaction of climate warming and increasing CO2 concentrations on nitrogen and carbon

cycling will determine future trends in NHL soil N2O emissions.

Soil nitrous oxide emissions across the northern high latitudes

Naiqing Pan[1], Hanqin Tian[1,2*], Hao Shi[3], Shufen Pan[4,1], Josep G. Canadell[5], Jinfeng Chang[6], Philippe Ciais[7], Eric A. Davidson[8], Gustaf Hugelius[9,10], Akihiko Ito[11], Robert B. Jackson[12], Fortunat Joos[13], Sebastian Lienert[13], Dylan B. Millet[14], Stefan Olin[15], Prabir K. Patra[16], Rona L. Thompson[17], Nicolas Vuichard[7], Kelley C. Wells[14], Chris Wilson[18,19], Yongfa You[1], Sönke Zaehle[20]

[1]Center for Earth System Science and Global Sustainability, Schiller Institute for Integrated Science and Society, Boston College, Chestnut Hill, MA, USA

[2]Department of Earth and Environmental Sciences, Boston College, Chestnut Hill, MA, USA

[3]State Key Laboratory of Urban and Regional Ecology, Research Center for Eco-Environmental Sciences, Chinese Academy of Sciences, Beijing, China

[4]Department of Engineering and Environmental Studies Program, Boston College, Chestnut Hill, MA, USA

5Global Carbon Project, CSIRO Oceans and Atmosphere, Canberra, Australian Capital Territory, Australia

[6] College of Environmental and Resource Sciences, Zhejiang University, Hangzhou, China

[7]Laboratoire des Sciences du Climat et de l'Environnement, LSCE, CEA CNRS, UVSQ UPSACLAY, Gif sur Yvette, France

[8]Appalachian Laboratory, University of Maryland Center for Environmental Science, Frostburg, MD, USA

[9]Department of Physical Geography, Stockholm University, Stockholm, Sweden

[10] Bolin Centre for Climate Research, Stockholm University, Stockholm, Sweden

[11] National Institute for Environmental Studies, Tsukuba, Japan

[12] Department of Earth System Science, Woods Institute for the Environment, Precourt Institute for Energy, Stanford University, Stanford, CA, USA

[13] Climate and Environmental Physics, Physics Institute and Oeschger Centre for Climate Change Research, University of Bern, Bern, Switzerland

[14] Department of Soil, Water, and Climate, University of Minnesota, St Paul, MN, USA

[15] Department of Physical Geography and Ecosystem Science, Lund University, Lund, Sweden

[16] Research Institute for Global Change, JAMSTEC, Yokohama, Japan

[17] Norsk Institutt for Luftforskning, NILU, Kjeller, Norway

[18] National Centre for Earth Observation, University of Leeds, Leeds, UK

[19] Institute for Climate and Atmospheric Science, School of Earth & Environment, University of Leeds, Leeds, UK

[20] Max Planck Institute for Biogeochemistry, Jena, Germany

*Corresponding author: Hanqin Tian (hanqin.tian@bc.edu)

Geophysical Research Letters (Submitted on January 18, 2024)

Abstract

Nitrous oxide (N_2O) is the most important stratospheric ozone-depleting agent based on current emissions and the third largest contributor to increased net radiative forcing. Increases in atmospheric N_2O have been attributed primarily to enhanced soil N_2O emissions. Critically, contributions from soils in the Northern High Latitudes (NHL, >50°N) remain poorly quantified despite their vulnerability to permafrost thawing induced by climate change. An ensemble of six terrestrial biosphere models suggests NHL soil N_2O emissions doubled since the preindustrial 1860s, increasing on average by 2.0±1.0 Gg N yr^{-1} (p<0.01). This trend reversed after the 1980s because of reduced nitrogen fertilizer application in non-permafrost regions and increased plant growth due to CO_2 fertilization suppressed emissions. However, permafrost soil N_2O emissions continued increasing attributable to climate warming; the interaction of climate warming and increasing CO_2 concentrations on nitrogen and carbon cycling will determine future trends in NHL soil N_2O emissions.

Key Points

1. N_2O emissions from northern high latitudes during 1997-2014 are estimated at 0.5–1.3 Tg N yr^{-1}, and soil was the largest source.

2. Northern high latitudes soil N_2O emissions increased from 0.3±0.1 Tg N yr^{-1} in 1861 to 0.6±0.3 Gg N yr^{-1} in 2016.

3. Climate change stimulated soil N_2O emissions, while the increased atmospheric CO_2 concentration suppressed emissions.

Plain Language Summary

Soils in the Northern High Latitudes (NHL) store large amounts of nitrogen, providing rich substrates for the emissions of nitrous oxide (N_2O) which is a potent greenhouse gas and ozone-depleting substance. The NHL has experienced rapid climate warming in recent decades, however, to what extent climate and other environmental factors have affected soil N cycling and N_2O emissions in the NHL remain poorly quantified. This study has provided the first quantification of the magnitudes and spatiotemporal variations of soil N_2O emissions across the NHL and showed that the NHL contributed about 8% of the increase in global soil N_2O emissions since pre-industrial period (the 1860s). Our results further reveal that changes in climate and atmospheric CO_2 concentration not only largely affected historical variations in soil N_2O emissions from the NHL but also will determine their future trends. Our study suggests the need to better understand climate and CO_2 controls on soil N_2O emissions and nitrogen cycling across the NHL and to improve their representation in earth system models.

1 Introduction

Nitrous oxide (N_2O) emissions have received increasing attention, because N_2O is the most important stratospheric ozone-depleting agent based on current emissions [*Ravishankara et al.*, 2009] and the third largest contributor to net radiative forcing by greenhouse gases [*Canadell et al.*, 2021; *Etminan et al.*, 2016]. The large amount of nitrogen additions to soils since the preindustrial period has significantly increased the atmospheric N_2O burden [*Canadell et al.*, 2021; *Tian et al.*, 2020]. Denitrification and nitrification are two primary soil processes controlling N_2O production, which are regulated by multiple factors such as temperature, water availability, acidity, substrate availability and microbial diversity [*Butterbach-Bahl et al.*, 2013; *Rees et al.*, 2013].

Over the past 40 years, the northern high latitudes, usually defined as the region north of 50°N [*Watts et al.*, 2012], have experienced climate warming at a rate faster than anywhere else on Earth [*Rantanen et al.*, 2022], a trend expected to continue in the coming decades [*Masson-Delmotte et al.*, 2021]. Therefore, there is an urgent need to understand and quantify how changes in climate and other environmental factors since the pre-industrial era have affected soil N_2O emissions from the NHL and thus have shaped the strength of climate-biogeochemical feedback.

The terrestrial nitrogen cycle in the NHL is closely related with permafrost, which underlays more than 60% of the area [*Brown et al.*, 1997]. Although large N stocks are stored in this region [*Harden et al.*, 2012; *Hugelius et al.*, 2020], the associated soil N_2O emissions have received little attention because they were considered to be small due to limited microbial activity and low mineralization rates under low-temperature and waterlogged conditions [*Voigt et al.*, 2020]. However, recent in-situ studies found that both barren and vegetated soils in the NHL can emit substantial amounts of N_2O [*Marushchak et al.*, 2011; *Marushchak et al.*, 2021; *Repo et al.*, 2009; *Voigt et al.*, 2017b]. Meanwhile, Arctic amplification, the phenomenon that climate change is amplified in the NHL, is projected to continue in the 21th century [*Christensen et al.*, 2013; *Pithan and Mauritsen*, 2014] with further implications for N_2O emissions: first, a large amount of immobile N stored in permafrost becomes available for decomposition and remobilization after permafrost thawing; second, rapid warming enhances N mineralization and promotes nitrification and denitrification; and third, warming may also promote biological nitrogen fixation (BNF), increasing ecosystem N availability and thereby potentially also N_2O production. Field experiments also confirm that warming can significantly increase N_2O emissions from permafrost-affected soils [*Cui et al.*, 2018; *Voigt et al.*, 2017b; *Wang et al.*, 2017].

Another influential factor for N_2O emissions in the NHL is the atmospheric CO_2 concentrations. Elevated atmospheric CO_2 concentrations do not have significant direct effects on reactive N flows controlling N_2O production, but can indirectly affect soil N_2O emissions by changing plant nitrogen uptake and root exudates due to enhanced plant growth [*Usyskin-Tonne et al.*, 2020]. On one hand, elevated atmospheric CO_2 promotes plant growth and thus more absorption of soil mineral N, restricting N_2O production [*Tian et al.*, 2019]. On the other hand, it may stimulate denitrification-derived N_2O emissions by increasing plant biomass and hence carbon substrate availability [*Kammann et al.*, 2008]. Additionally, elevated CO_2 can affect soil moisture by improving plant water-use efficiency, which can increase anaerobic conditions that stimulate denitrification [*Butterbach-Bahl et al.*, 2013]. Such contrasting effects of elevated CO_2 concentrations on N_2O emissions have been observed in field experiments [*Dijkstra et al.*, 2012; *Liu et al.*, 2018; *X Sun et al.*, 2018] but the magnitude of the CO_2 effect on northern soil N_2O emissions remains poorly understood.

Here, we investigated NHL soil N_2O emissions using six process-based terrestrial biosphere models (TBMs) from the global N_2O Model Intercomparison Project (NMIP) [*Tian et al.*, 2018]. Using factorial simulation experiments, we quantified the contributions of different driving factors, particularly climate change and rising atmospheric CO_2, to the variations in soil N_2O emissions during 1861-2016. Statistical methods were further employed to disentangle the effects of temperature and precipitation on soil N_2O emissions. We also compared bottom-up (BU, including process-based TBMs for soil emissions and emission factor approaches for non-soil emissions) estimates of N_2O emissions with those of three atmospheric inversion frameworks (top-down, TD) [*Rona L. Thompson et al.*, 2019] to investigate the uncertainties in current estimates of N_2O emissions from the NHL.

2 Materials and methods

2.1 Data sources

2.1.1 Soil N_2O emissions

An ensemble estimate of soil N_2O emissions from the NHL was derived from simulations by the six TBMs that participated in the NMIP: (1) DLEM [*Tian et al.*, 2015], (2) LPJ-GUESS [*Olin et al.*, 2015], (3) LPX-Bern [*Joos et al.*, 2020], (4) O-CN [*Zaehle et al.*, 2011], (5) ORCHIDEE-CNP [*Goll et al.*, 2017; *Y Sun et al.*, 2021], and (6) VISIT [*Inatomi et al.*, 2010]. Each model performed a subset of seven simulations (S0-S6) to quantify N_2O emissions from both agricultural and natural soils, and to disentangle the effects of multiple environmental factors on N_2O emissions (Table S1). The differences between pairs of simulations, i.e. S1-S2, S2-S3, S3-S4, S4-S5, S5-S6, and S6-S0, were used to evaluate the effects of manure N, mineral N fertilizer, atmospheric N deposition, land use and land cover change (LULCC), atmospheric CO_2 concentration, and climate, respectively. More information about the model simulation protocol and forcing data can refer to *Tian et al.* [2018]. Among the six NMIP models, LPJ-GUESS and LPX-Bern have dedicated permafrost modules and consider freeze-thaw processes; O-CN lacks an explicit permafrost representation but describes freeze-thaw cycles; the other models have no explicit representation of the permafrost layer or freeze-thaw processes.

2.1.2 Fire-induced N_2O emissions and non-soil anthropogenic N_2O emissions

N_2O emissions from biomass burning were from the GFED4.1s dataset. N_2O emissions from non-soil anthropogenic sources were obtained from EDGAR 6.0 [*Crippa et al.*, 2019]. EDGAR non-soil anthropogenic emissions were combined with GFED biomass burning emissions and with

NMIP soil emissions to constitute BU estimates of total N_2O emissions, aiming to make comparison with TD estimates.

2.1.3 Top-down N_2O emission estimates

Three independent atmospheric inversion models were used: GEOS-Chem [*Wells et al.*, 2018], INVICAT [*Wilson et al.*, 2014] and MIROC4-ACTM [*Patra et al.*, 2018; *Patra et al.*, 2022]. GEOS-Chem and INVICAT used the same prior estimates: soil emissions from the O-CN model, biomass burning emissions from GFEDv4.1s, and non-soil anthropogenic emissions from EDGAR v4.2FT2010. The MIROC4-ACTM prior used natural soil emissions from the VISIT model, and all anthropogenic emissions from EDGAR 4.2. The MIROC4-ACTM prior included agricultural burning but did not explicitly include wildfire emissions. All models used the Bayesian inversion framework to find the optimal emissions that provide the best agreement to observed N_2O mixing ratios while being coupled to an atmospheric transport model.

2.2 Statistical methods

The path analysis model (PAM) was used to investigate how climatic factors affected permafrost soil N_2O emissions. PAM can deal with complex relationships among multiple independent and dependent variables, and disentangle direct and indirect effects of the explanatory variables on the response variable [*Alwin and Hauser*, 1975; *You and Pan*, 2020]. Here, we developed the conceptual model by specifying the relationships between climatic factors and soil N_2O emissions and considering the interactions between these factors. We also conducted partial correlation analysis between soil N_2O emissions and temperature/precipitation. The temporal sensitivities of soil N_2O emissions to temperature and precipitation were fitted using a multiple regression model. The Mann–Kendall test was used to assess the significance of trends in N_2O emissions.

3 Results

3.1 Spatiotemporal variations of soil N_2O emissions since the 1860s

Multi-model ensemble estimates show that soil N_2O emissions from the NHL increased from 312±125 Gg N yr^{-1} in 1861 to 605±269 Gg N yr^{-1} in 2016 (Fig.1a), with an average increase rate of 2.0±1.0 Gg N yr^{-1} (p<0.01). Soil N_2O emissions from non-permafrost regions dominated the temporal variations of total NHL emissions, which were relatively stable over the first five decades, then rapidly increased from the 1920s to the 1980s, and peaked in the 1980s. In the late 1980s and early 1990s, northern soil N_2O emissions drastically decreased and fluctuated afterwards. Meanwhile, soil N_2O emissions from permafrost regions showed different temporal dynamics; they remained relatively stable before the 1980s, and rapidly increased thereafter. In the 1860s, the highest emission density occurred in Central Europe. During 1861-2016, soil N_2O emissions from most regions significantly increased. In the recent decade (2007-2016), Western Europe had the highest emission density (Fig.1b-d), and more than half of the soil N_2O emissions were from croplands (Fig. S2). During 1861-1980, the fastest increase in N_2O emissions occurred in Western and Central Europe where the average increase exceeded 2×10^{-4} g N m^{-2} yr^{-1} (Fig.1e). However, trends in soil N_2O emissions have largely changed since 1980, with emissions significantly decreasing in Eastern Europe and Russia but rapidly increasing in Siberia and Southern Canada (Fig.1f).

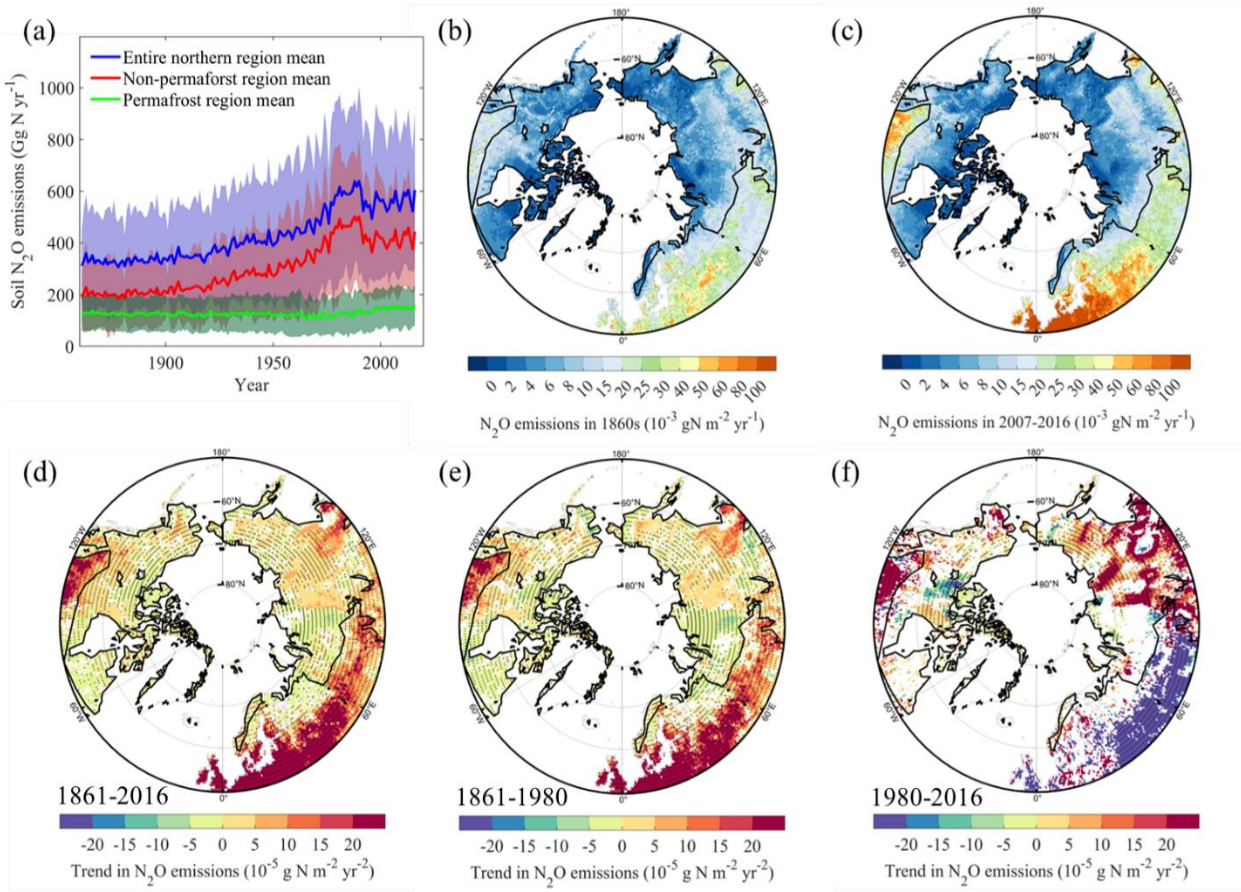

Fig. 1: (a) Changes in soil N_2O emissions from the NHL, the shaded area indicates one standard deviation of all estimates. (b) and (c) show spatial pattern of mean annual soil N_2O emissions during the 1860s and 2007-2016, respectively. Trends in soil N_2O emissions during 1861-2016 (d), 1861-1980 (e), and 1980-2016 (f); grids with non-significant trends (p>=0.05) were excluded, and stippling indicates where a majority of models (at least 4 out of 6) agree on the sign of the trend.

3.2 Contributions of different driving factors to soil N_2O emissions during 1861-2016

Our results derived from factorial simulations suggested that increasing atmospheric CO_2 concentrations reduced NHL soil N_2O emissions, while the other five factors stimulated N_2O emissions (Fig. 2a). Climate change played a dominant role in stimulating N_2O emissions before the 1930s and N inputs made increasing contributions from the 1940s to the 1980s. From the 1860s to the 1980s, fertilizer application contributed 53% to the increase in emissions, followed by atmospheric N deposition (26%), manure N application (15%), climate change (12%), and land use change (5%). The effect of increased atmospheric CO_2 (-10%) almost offset that of climate change. Since the 1980s, the role of anthropogenic N inputs in stimulating N_2O emissions weakened gradually; by contrast, drastic warming and wetting made climate change increasingly important (Fig. S3). Over the entire study period, climate change made the second largest contribution (37%) to the increase of NHL soil emissions after N fertilizer application (42%). Climate change had a larger relative contribution to the emission increase in permafrost regions (Fig. 2c) than in non-permafrost regions. During 1861-2016, climate change contributed 114% (partly offset by the negative CO_2 effect) to the emission increase in permafrost regions, which was stronger than in non-permafrost regions (28%) (Fig. 2d). All individual models agreed that climate change made a larger relative contribution to emission increases in permafrost regions than in non-permafrost regions, and that the effects of climate change have increased since the 1980s (Fig. S4-6). In most northern regions, trends in soil N_2O emissions were dominated by climate change; fertilizer only dominated trends in Western Europe and some intensive agricultural lands over Eastern Europe, Russia, and south Canada, while atmospheric N deposition dominated trends in part of Central and Eastern Europe. Regions dominated by other factors were relatively small (Fig. 2b).

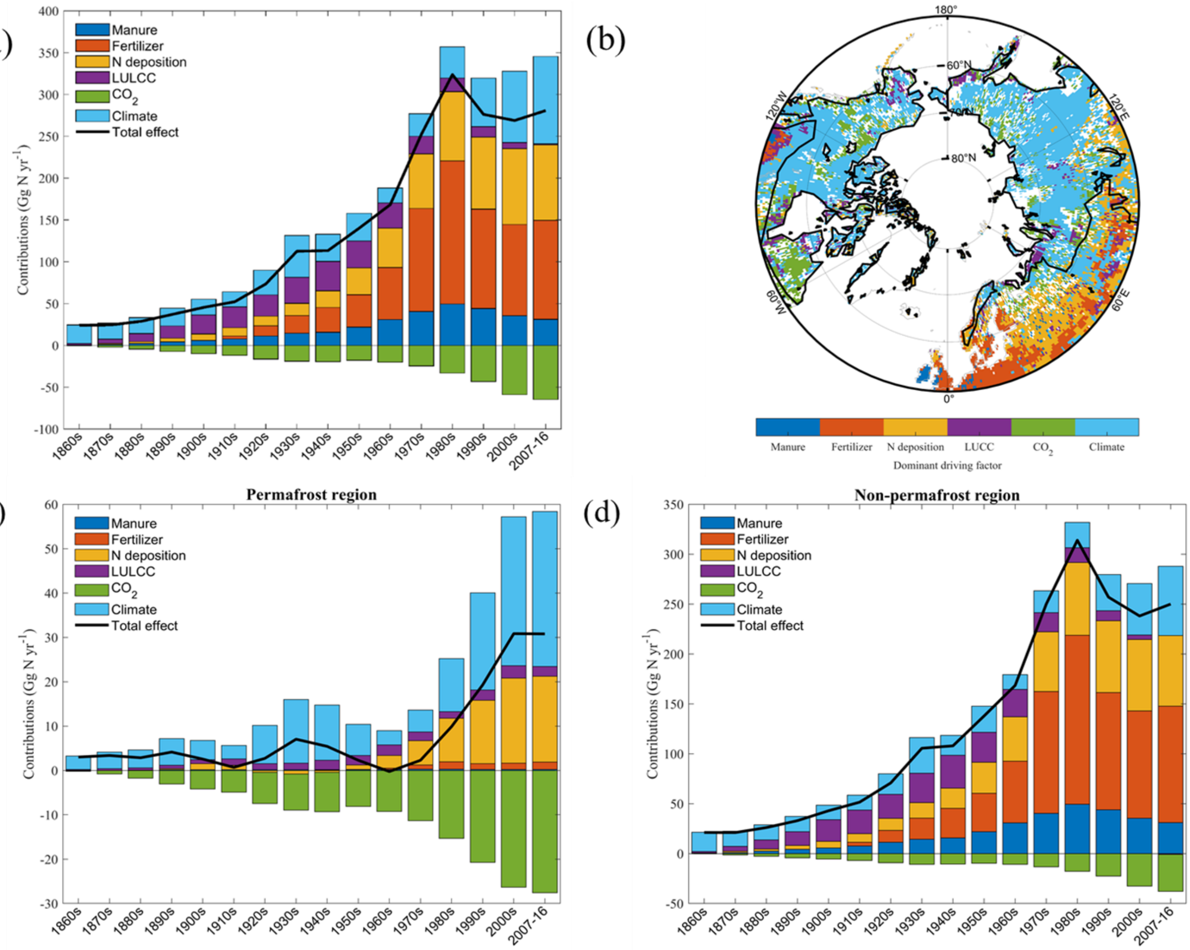

Fig. 2: (a) Decadal variations in the contributions of different driving factors. (b) Distribution of dominant driving factors of soil N_2O emissions during 1861-2016; grids with non-significant trends were excluded. Contributions of different driving factors to soil N_2O emissions from permafrost regions (c) and non-permafrost regions (d).

3.3 Effects of temperature and precipitation on soil N_2O emissions

Temperature and precipitation changes alter soil microclimate , nutrient availability and microbial ecology , thereby influencing N_2O emissions [*Dalal and Allen*, 2008]. For the entire NHL, both temperature and precipitation significantly increased during 1901-2016, with rates of 0.14 ℃ per decade and 0.38 mm yr^{-1} (10% total increase since the 1900s), respectively (Fig. S3). According to multiple regression model results, the sensitivities of soil N_2O emissions to temperature and precipitation were 29±21 Gg N °C^{-1} and 0.4±0.7 Gg N mm^{-1} during 1901-2016, suggesting that warming and wetting increased soil N_2O emissions by 48±35 Gg N yr^{-1} and 15±26 Gg N yr^{-1}, respectively. The path analysis model also suggested that warming contributed more to soil N_2O emission increases than wetting (Fig. S7). Both warming and wetting have accelerated since 1980 (Fig. S3, S8, S9), with average rates of 0.38 °C per decade and 0.57 mm yr^{-2}, respectively. At the same time, the sensitivities of soil N_2O emissions to temperature and precipitation increased to 38±22 Gg N °C^{-1} and 1.2±0.8 Gg N mm^{-1}, respectively. These two factors together led to the large climate effects in the recent four decades.

Soil N_2O emissions were positively correlated with temperature in most northern regions (Fig. S10a). Compared with the 1901-1980 period, warming after 1980 was more pronounced and prevalent (Fig. S8-9), which enhanced biological N fixation and net N mineralization and further promoted nitrification and denitrification (Fig. S11). During the study period, most of the NHL experienced significant warming (Fig. S10c), indicating that warming universally stimulated N_2O emissions in this region. Recent manipulation experiments also suggest that warming can significantly increase soil N_2O emissions from the NHL [*Cui et al.*, 2018; *Voigt et al.*, 2017b; *Wang et al.*, 2017]. Unlike temperature, the correlation between soil N_2O emissions and precipitation varied spatially (Fig. S10b). Although a large area of the NHL experienced significant wetting (Fig. S10d), the positive effects of wetting on emissions from Eastern Europe, central Canada and Siberia were partly counteracted by the negative effects in Northern Europe and northwestern Russia, which explained why precipitation had a smaller effect than temperature on the regional total emissions.

3.4 Declining soil N_2O emissions since the 1980s

Soil N_2O emissions from the NHL rapidly increased before the 1980s, however, declined thereafter. Although total BNF over the NHL increased since 1980 (Fig. S12), the ensemble mean of soil N_2O emissions from the NHL decreased at an average rate of -1.1 GgN yr^{-1} ($p<0.05$) during 1980-2016 (Fig. 3a). The rapid decline in emissions during 1988-1996 was due to reduced fertilizer application, after which period the negative effect of CO_2 fertilization was enhanced (Fig. S14). The most pronounced decline occurred in Eastern Europe and Russia (Fig. 1f), mainly caused by the sharp decrease in external nitrogen inputs due to the collapse of the Soviet Union (Fig. S14). Concurrently, soil emissions from Siberia and Southern Canada significantly increased, due to climate change and nitrogen enrichment, respectively (Fig. S14). Soil N_2O emissions fluctuated after 1998 because the positive climate effect was counteracted by combined effects of fertilizer application, CO_2 and land use change.

The dominant drivers of negative effects differed between permafrost and non-permafrost regions. In permafrost regions, elevated CO_2 concentration was the only factor suppressing soil N_2O emissions and counteracted more than half of the climate-induced emissions (Fig. 3b). By contrast, reduced N fertilizer application, elevated CO_2 concentration and land use change jointly reduced emissions from non-permafrost regions (Fig. 3c). For the entire NHL, the atmospheric CO_2-induced decline in soil N_2O emissions surpassed the effect of reduced fertilizer application over the recent decade. Elevated atmospheric CO_2 significantly suppressed N_2O emissions in most northern regions (Fig. S14). Since the 1980s, increased atmospheric CO_2 concentrations stimulated terrestrial gross primary production (Fig. S15a, c), thus enhancing plant nitrogen uptake (Fig. S15b, d) and reducing the availability of soil inorganic nitrogen, which finally suppressed N_2O emissions.

The largest stimulation effect of CO_2 on vegetation growth and nitrogen uptake occurred in the boreal forests, where the CO_2-induced suppression of N_2O emissions was the most pronounced. Enhanced vegetation growth in the NHL has been reported in previous studies [*Berner et al.*, 2020; *Myers-Smith et al.*, 2020; *Virkkala et al.*, 2021]. Reduced N_2O emissions due to enhanced plant growth and nitrogen uptake is also consistent with field observations in the NHL [*Gong and Wu*, 2021; *Marushchak et al.*, 2011; *Stewart et al.*, 2012].

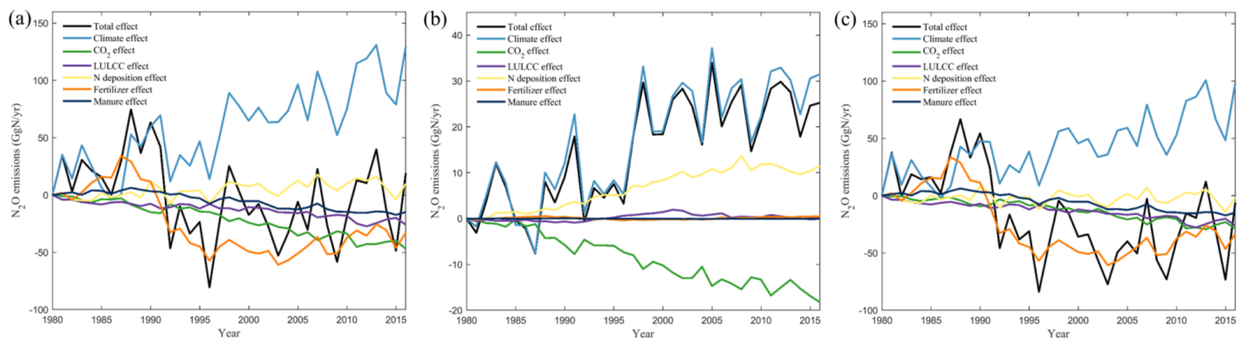

Fig. 3: Contributions of different driving factors in the entire NHL (a), permafrost regions (b), and non-permafrost regions (c) during 1980-2016.

3.5 Comparison with TD estimates

Using the current N_2O observation network, TD models estimate total N_2O emissions with its spatial distribution across the land but cannot well quantify the contributions of different sources. With the aim of comparing BU estimates with TD estimates, we added N_2O emissions from soil, biomass burning and non-soil anthropogenic sources (Fig. S16) together to constitute BU estimates of total N_2O emissions. According to the resulting BU estimates, soil was the largest source of N_2O emissions in the NHL (mean value: 572 Gg N yr^{-1} during 1998-2014), followed by non-soil anthropogenic sources (280 Gg N yr^{-1}) and biomass burning (143 Gg N yr^{-1}). Both BU and TD approaches indicated similar spatial emission patterns (Fig. 4), but the ensemble mean of total BU estimate (995±267 Gg N yr^{-1}) was substantially higher than the TD estimate (668±134 Gg N yr^{-1}) for the overlapping 1998-2014 period. Both TD and BU approaches revealed that the total N_2O emissions had no significant trend during this period (p>0.05). Removing N_2O emitted by biomass burning and non-soil anthropogenic sources from the TD estimates, the remaining N_2O exhibited a decreasing trend during 1998-2014 (from -10.0 to -3.2 Gg N yr^{-2}, mean -7.3 Gg N yr^{-2}), implying that the TD models also suggest a decreasing trend in NHL soil N_2O emissions.

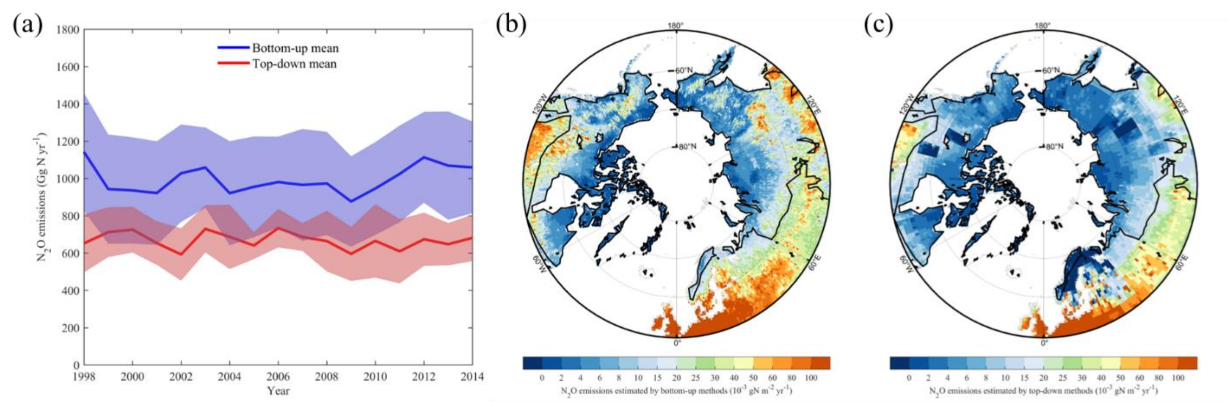

Fig. 4: (a) Comparison between TD and BU estimates of total N_2O emissions, the lines represent the ensemble means and the shaded areas indicate one standard deviation of model estimates. Spatial pattern of total N_2O emissions estimated by BU (b) and TD (c) approaches.

3.6 Comparison with empirical estimates

Based on site-level observation data, *Voigt et al.* [2020] estimated soil N_2O emissions from permafrost regions using a simple extrapolation method, and proposed that peatlands had the highest N_2O emissions among natural permafrost ecosystems. However, these extrapolation-based estimates have large uncertainties, with the implied annual soil N_2O emissions from the NHL ranging from 140 to 1030 Gg N^{-1}. In particular, estimates based on mean fluxes are an order of magnitude larger than those based on median fluxes because of several N_2O emission hot spots. Combining observed peatland annual fluxes and peatland distribution maps, *Hugelius et al.* [2020] estimated a much smaller northern peatland source of 22 ± 5 Gg $N \cdot y^{-1}$, with only half of that peatland area being permafrost. This suggests a smaller source than the estimates of *Voigt et al.* [2020]. NMIP estimates of soil N_2O emissions from the permafrost regions are close to the lower-limit of estimates by *Voigt et al.* [2020], and have smaller uncertainty range (0.11-0.26 Tg N^{-1}, mean 0.17 Tg N^{-1}), which partly reflect the usage of unified model input data. Soil N_2O emissions from non-permafrost regions are largely controlled by fertilizer and manure applications. According to NMIP models, the average emission factors of fertilizer and manure in non-permafrost regions during 1980-2016 were 1.4% and 1.7%, respectively. Both factors were positively correlated with temperature and precipitation, suggesting positive interactions between nitrogen additions and climate change [*Tian et al.*, 2020].

4 Discussion

Our study provides a first estimate of soil N_2O emissions from the NHL, although large uncertainties remain in both TD and BU approaches (Fig. S17, S18). Since the process-based models used in this study were driven by the same input data, differences were mainly induced by missing or uncertain representation of important processes such as seasonal freeze-thaw cycles and permafrost thaw [*Risk et al.*, 2013], BNF [*Meyerholt et al.*, 2020] and reactive N flows through ecosystems [*Butterbach-Bahl et al.*, 2013], and critical information such as timing and frequency of fertilizer application [*Nishina et al.*, 2017]. Several NMIP models do not include an explicit permafrost layer or freeze-thaw processes; inclusion of such factors would enable better representation of "hot spots" and "hot moments" soil N_2O emissions in the NHL [*Voigt et al.*, 2020;

Wagner-Riddle et al., 2017]. Current process-based TBMs also have insufficient representation of the upland thermokarst formation [*Yang et al.*, 2018] and fine-grained landscape structure of arctic ecosystems (e.g., landscape elements that are ultra-emitters of N_2O such as non-vegetated organic soil). Integrating sub-grid scale information and processes into models may provide a solution for fine-grained physical-hydrological modelling. As revealed by *Voigt et al.* [2020], peatlands have the highest N_2O emission rate in permafrost regions. It is thus important for process-based TBMs to explicitly consider peatland thermal, hydrological, and biogeochemical processes.

TD estimates have a stronger dependence on the prior fluxes in NHL where atmospheric N_2O measurements are sparse [*Nevison et al.*, 2018; *Rona Louise Thompson et al.*, 2014; *Rona L. Thompson et al.*, 2019]. In this study, the average prior N_2O flux employed in the TD models (846±141 Gg N yr^{-1}) was lower than our BU estimates (955±267 Gg N yr^{-1}). These low prior N_2O fluxes, as well as lower TD emissions in summer compared to the BU estimates, are the likely causes of the lower TD estimates (Fig. S18). Differing prior N_2O fluxes between the inversions (see methods) also lead to somewhat varying inversion estimates. Using the ensemble mean NMIP soil emission estimates as prior for the TD inversions may improve model agreement. The total prior ocean flux also has important impacts on the magnitude of the terrestrial flux. However, there have been few observational constraints on the ocean source until recently [*Patra et al.*, 2022]. The sparseness of atmospheric observations over both land and ocean north of 50°N and systematic model errors in stratosphere-troposphere exchange increase the uncertainty in TD estimates. Building denser regional N_2O monitoring networks and launching (regular) aircraft campaigns in the NHL will help better constrain inversion models [*Bisht et al.*, 2021].

Our results suggest that the NHL contributed approximately 8% of the increase in global soil N_2O emissions during 1861-2016 [*Tian et al.*, 2019]. Warming and wetting stimulated NHL soil N_2O emissions, while elevated CO_2 concentrations suppressed emissions (through increased plant growth and larger uptake of soil N), findings that are in line with field observations [*Cui et al.*, 2018; *Dijkstra et al.*, 2012; *Gong and Wu*, 2021; *Marushchak et al.*, 2011; *Voigt et al.*, 2017a]. From 1980-2016 when warming was strongest, the NHL contributed 14% of global climate effect enhancing soil N_2O emissions. Under the SSP370 and SSP585 scenarios, CMIP6 climate models predict that the mean temperature of the NHL will increase by 6.2 (4.1-9.8) °C and 7.8 (5.5-12.1) °C, respectively, during 2015-2100; the mean precipitation will increase by 96（65-177）mm yr^{-1} and 129（51-206）mm yr^{-1}, respectively (Fig. S19). If the sensitivities of soil N_2O emissions to temperature and precipitation in the future are consistent with historical values, future climate change alone will substantially increase NHL soil N_2O emissions. However, atmospheric CO_2 concentrations also rapidly increase under SSP370 and SSP585 scenarios (Fig. S20), potentially offsetting a significant fraction of the positive climate effect if arctic vegetation continues to take up more carbon and nitrogen with elevated CO_2. Uncertainties arise regarding the degree of recycling of that extra nitrogen uptake in soils by mineralization. The magnitude of the future CO_2 effect is also highly uncertain [*Walker et al.*, 2021], and how it will affect future northern N_2O emissions requires further study. Reconstructions from ice cores show that global N_2O emissions increased over the last deglaciation when the climate warmed, CO_2 increased, and land carbon inventories grew in size, providing evidence for a net positive relationship between past warming, CO_2, land carbon, stocks, and N_2O emissions at the global scale [*Fischer et al.*, 2019; *Joos et al.*, 2020].

Since the NMIP project did not design simulation experiments to separate the effects of temperature and precipitation on soil N_2O emissions, we used statistical methods to explore these relationships. However, the collinearity between temperature and precipitation variations may undermine the reliability of the inferred sensitivities of soil N_2O emissions to temperature and precipitation. Future model intercomparison projects need to design simulations to disentangle the effects of temperature and precipitation.

Acknowledgements

This study was resulted from NMIP (global N/N2O Model Intercomparison Project) co-sponsored by Global Carbon Project and International Nitrogen Initiative. This work contributes to the REgional Carbon Cycle Assessment and Porcesses-2 of the Global Carbon Project. H.T., N. Pan, S. Pan acknowledge funding support from NSF (grant nos. 1903722, 1922687); PKP is partly funded by the Arctic Challenge for Sustainability phase II (ArCS-II; JPMXD1420318865) Projects of the Ministry of Education, Culture, Sports, Science and Technology (MEXT); KCW and DBM acknowledge support from NASA (Grant #NNX17AK18G) and NOAA (Grant #NA13OAR4310086).

Data availability statement

EDGAR 6.0 dataset is available at https://edgar.jrc.ec.europa.eu/dataset_ghg60. GFED4.1s dataset is available at https://www.geo.vu.nl/~gwerf/GFED/GFED4/. Soil N_2O emissions, terrestrial GPP and plant nitrogen uptake estimated by NMIP models and top-down N_2O emission are available at https://datadryad.org/stash/share/isclqpURaZ5GJLLok3LCvjBrQ20ybXX7M3dQzuVWFCk

Author contributions

H.T. initiated and designed this research, N.P. conducted data analysis and synthesis, N.P. and H.T. drafted the manuscript. All co-authors contributed to the writing and development of the manuscript.

Competing interests

The authors declare no competing interests.

References

Alwin, D. F., and R. M. Hauser (1975), The decomposition of effects in path analysis, *American sociological review*, 37-47.

Berner, L. T., R. Massey, P. Jantz, B. C. Forbes, M. Macias-Fauria, I. Myers-Smith, T. Kumpula, G. Gauthier, L. Andreu-Hayles, and B. V. Gaglioti (2020), Summer warming explains widespread but not uniform greening in the Arctic tundra biome, *Nature communications*, *11*(1), 1-12.

Bisht, J. S. H., T. Machida, N. Chandra, K. Tsuboi, P. K. Patra, T. Umezawa, Y. Niwa, Y. Sawa, S. Morimoto, and T. Nakazawa (2021), Seasonal Variations of SF6, CO2, CH4, and N2O in the UT/LS Region due to Emissions, Transport, and Chemistry, *Journal of Geophysical Research: Atmospheres*, *126*(4), e2020JD033541.

Brown, J., O. J. Ferrians Jr, J. A. Heginbottom, and E. S. Melnikov (1997), Circum-arctic map of permafrost and ground ice conditions.

Butterbach-Bahl, K., L. Baggs, M. Dannenmann, R. Kiese, and S. Zechmeister-Boltenstern (2013), Nitrous oxide emissions from soils: How well do we understand the processes and their controls?, *Philosophical transactions of the Royal Society of London. Series B, Biological sciences*, *368*, 20130122.

Canadell, J. G., P. M. S. Monteiro, M. H. Costa, L. C. Da Cunha, P. M. Cox, V. Alexey, S. Henson, M. Ishii, S. Jaccard, and C. Koven (2021), Global carbon and other biogeochemical cycles and feedbacks, edited.

Christensen, J. H., K. K. Kanikicharla, E. Aldrian, S. I. An, I. F. A. Cavalcanti, M. de Castro, W. Dong, P. Goswami, A. Hall, and J. K. Kanyanga (2013), Climate phenomena and their relevance for future regional climate change, in *Climate change 2013 the physical science basis: Working group I contribution to the fifth assessment report of the intergovernmental panel on climate change*, edited, pp. 1217-1308, Cambridge University Press.

Crippa, M., G. Oreggioni, D. Guizzardi, M. Muntean, E. Schaaf, E. Lo Vullo, E. Solazzo, F. Monforti-Ferrario, J. G. J. Olivier, and E. Vignati (2019), Fossil CO2 and GHG emissions of all world countries, *Publication Office of the European Union: Luxemburg*.

Cui, Q., C. Song, X. Wang, F. Shi, X. Yu, and W. Tan (2018), Effects of warming on N2O fluxes in a boreal peatland of Permafrost region, Northeast China, *Science of The Total Environment*, *616-617*, 427-434.

Dalal, R. C., and D. E. Allen (2008), Greenhouse gas fluxes from natural ecosystems, *Australian Journal of Botany*, *56*(5), 369-407.

Dijkstra, F. A., S. A. Prior, G. B. Runion, H. A. Torbert, H. Tian, C. Lu, and R. T. Venterea (2012), Effects of elevated carbon dioxide and increased temperature on methane and nitrous oxide fluxes: evidence from field experiments, *Frontiers in Ecology and the Environment*, *10*(10), 520-527.

Etminan, M., G. Myhre, E. J. Highwood, and K. P. Shine (2016), Radiative forcing of carbon dioxide, methane, and nitrous oxide: A significant revision of the methane radiative forcing, *Geophysical Research Letters*, *43*(24), 12-614.

Fischer, H., et al. (2019), N2O changes from the Last Glacial Maximum to the preindustrial – Part 1: Quantitative reconstruction of terrestrial and marine emissions using N2O stable isotopes in ice cores, *Biogeosciences*, *16*(20), 3997-4021.

Goll, D. S., et al. (2017), A representation of the phosphorus cycle for ORCHIDEE (revision 4520), *Geosci. Model Dev.*, *10*(10), 3745-3770.

Gong, Y., and J. Wu (2021), Vegetation composition modulates the interaction of climate warming and elevated nitrogen deposition on nitrous oxide flux in a boreal peatland, *Global Change Biology*, *27*(21), 5588-5598.

Harden, J. W., et al. (2012), Field information links permafrost carbon to physical vulnerabilities of thawing, *Geophysical Research Letters*, *39*(15).

Hugelius, G., J. Loisel, S. Chadburn, R. B. Jackson, M. Jones, G. MacDonald, M. Marushchak, D. Olefeldt, M. Packalen, and M. B. Siewert (2020), Large stocks of peatland carbon and nitrogen are vulnerable to permafrost thaw, *Proceedings of the National Academy of Sciences*, *117*(34), 20438-20446.

Inatomi, M., A. Ito, K. Ishijima, and S. Murayama (2010), Greenhouse gas budget of a cool-temperate deciduous broad-leaved forest in Japan estimated using a process-based model, *Ecosystems*, *13*(3), 472-483.

Joos, F., R. Spahni, B. D. Stocker, S. Lienert, J. Müller, H. Fischer, J. Schmitt, I. C. Prentice, B. Otto-Bliesner, and Z. Liu (2020), N_2O changes from the Last Glacial Maximum to the preindustrial – Part 2: terrestrial N_2O emissions and carbon–nitrogen cycle interactions, *Biogeosciences*, *17*(13), 3511-3543.

Kammann, C., C. Müller, L. Grünhage, and H.-J. Jäger (2008), Elevated CO2 stimulates N2O emissions in permanent grassland, *Soil Biology and Biochemistry*, *40*(9), 2194-2205.

Liu, S., C. Ji, C. Wang, J. Chen, Y. Jin, Z. Zou, S. Li, S. Niu, and J. Zou (2018), Climatic role of terrestrial ecosystem under elevated CO 2: a bottom ‐ up greenhouse gases budget, *Ecology letters*, *21*(7), 1108-1118.

Marushchak, M. E., A. PitkÄMÄKi, H. Koponen, C. Biasi, M. SeppÄLÄ, and P. J. Martikainen (2011), Hot spots for nitrous oxide emissions found in different types of permafrost peatlands, *Global Change Biology*, *17*(8), 2601-2614.

Marushchak, M. E., J. Kerttula, K. Diáková, A. Faguet, J. Gil, G. Grosse, C. Knoblauch, N. Lashchinskiy, P. J. Martikainen, and A. Morgenstern (2021), Thawing Yedoma permafrost is a neglected nitrous oxide source, *Nature communications*, *12*(1), 1-10.

Masson-Delmotte, V., P. Zhai, A. Pirani, S. L. Connors, C. Péan, S. Berger, N. Caud, Y. Chen, L. Goldfarb, and M. I. Gomis (2021), Climate Change 2021: The Physical Science Basis. Contribution of Working Group I to the Sixth Assessment Report of the Intergovernmental Panel on Climate Change, *IPCC: Geneva, Switzerland*.

Meyerholt, J., K. Sickel, and S. Zaehle (2020), Ensemble projections elucidate effects of uncertainty in terrestrial nitrogen limitation on future carbon uptake, *Global Change Biology*, *26*(7), 3978-3996.

Myers-Smith, I. H., J. T. Kerby, G. K. Phoenix, J. W. Bjerke, H. E. Epstein, J. J. Assmann, C. John, L. Andreu-Hayles, S. Angers-Blondin, and P. S. Beck (2020), Complexity revealed in the greening of the Arctic, *Nature Climate Change*, *10*(2), 106-117.

Nevison, C., A. Andrews, K. Thoning, E. Dlugokencky, C. Sweeney, S. Miller, E. Saikawa, J. Benmergui, M. Fischer, and M. Mountain (2018), Nitrous oxide emissions estimated with the CarbonTracker ‐ Lagrange North American regional inversion framework, *Global Biogeochemical Cycles*, *32*(3), 463-485.

Nishina, K., A. Ito, N. Hanasaki, and S. Hayashi (2017), Reconstruction of spatially detailed global map of NH4+ and NO3− application in synthetic nitrogen fertilizer, *Earth Syst. Sci. Data*, *9*(1), 149-162.

Olin, S., M. Lindeskog, T. A. M. Pugh, G. Schurgers, D. Wårlind, M. Mishurov, S. Zaehle, B. D. Stocker, B. Smith, and A. Arneth (2015), Soil carbon management in large-scale Earth system modelling: implications for crop yields and nitrogen leaching, *Earth System Dynamics*, *6*(2), 745-768.

Patra, P. K., M. Takigawa, S. Watanabe, N. Chandra, K. Ishijima, and Y. Yamashita (2018), Improved chemical tracer simulation by MIROC4. 0-based atmospheric chemistry-transport model (MIROC4-ACTM), *Sola*, *14*, 91-96.

Patra, P. K., E. J. Dlugokencky, J. W. Elkins, G. S. Dutton, Y. Tohjima, M. Sasakawa, A. Ito, R. F. Weiss, M. Manizza, and P. B. Krummel (2022), Forward and inverse modelling of atmospheric nitrous oxide using MIROC4-atmospheric chemistry-transport model, *Journal of the Meteorological Society of Japan. Ser. II*.

Pithan, F., and T. Mauritsen (2014), Arctic amplification dominated by temperature feedbacks in contemporary climate models, *Nature Geoscience*, *7*(3), 181-184.

Rantanen, M., A. Y. Karpechko, A. Lipponen, K. Nordling, O. Hyvärinen, K. Ruosteenoja, T. Vihma, and A. Laaksonen (2022), The Arctic has warmed nearly four times faster than the globe since 1979, *Communications Earth & Environment*, *3*(1), 168.

Ravishankara, A. R., J. S. Daniel, and R. W. Portmann (2009), Nitrous oxide (N2O): the dominant ozone-depleting substance emitted in the 21st century, *science*, *326*(5949), 123-125.

Rees, R. M., J. Augustin, G. Alberti, B. C. Ball, P. Boeckx, A. Cantarel, S. Castaldi, N. Chirinda, B. Chojnicki, and M. Giebels (2013), Nitrous oxide emissions from European agriculture–an analysis of variability and drivers of emissions from field experiments, *Biogeosciences*, *10*(4), 2671-2682.

Repo, M. E., S. Susiluoto, S. E. Lind, S. Jokinen, V. Elsakov, C. Biasi, T. Virtanen, and P. J. Martikainen (2009), Large N2O emissions from cryoturbated peat soil in tundra, *Nature Geoscience*, *2*(3), 189-192.

Risk, N., D. Snider, and C. Wagner-Riddle (2013), Mechanisms leading to enhanced soil nitrous oxide fluxes induced by freeze–thaw cycles, *Canadian Journal of Soil Science*, *93*(4), 401-414.

Stewart, K. J., M. E. Brummell, R. E. Farrell, and S. D. Siciliano (2012), N2O flux from plant-soil systems in polar deserts switch between sources and sinks under different light conditions, *Soil Biology and Biochemistry*, *48*, 69-77.

Sun, X., X. Han, F. Ping, L. Zhang, K. Zhang, M. Chen, and W. Wu (2018), Effect of rice-straw biochar on nitrous oxide emissions from paddy soils under elevated CO2 and temperature, *Science of the total environment*, *628*, 1009-1016.

Sun, Y., D. S. Goll, J. Chang, P. Ciais, B. Guenet, J. Helfenstein, Y. Huang, R. Lauerwald, F. Maignan, and V. Naipal (2021), Global evaluation of the nutrient-enabled version of the land surface model ORCHIDEE-CNP v1. 2 (r5986), *Geoscientific Model Development*, *14*(4), 1987-2010.

Thompson, R. L., K. Ishijima, E. Saikawa, M. Corazza, U. Karstens, P. K. Patra, P. Bergamaschi, F. Chevallier, E. Dlugokencky, and R. G. Prinn (2014), TransCom N 2 O model inter-comparison–Part 2: Atmospheric inversion estimates of N 2 O emissions, *Atmospheric Chemistry and Physics*, *14*(12), 6177-6194.

Thompson, R. L., L. Lassaletta, P. K. Patra, C. Wilson, K. C. Wells, A. Gressent, E. N. Koffi, M. P. Chipperfield, W. Winiwarter, and E. A. Davidson (2019), Acceleration of global N2O emissions seen from two decades of atmospheric inversion, *Nature Climate Change*, *9*(12), 993-998.

Tian, H., G. Chen, C. Lu, X. Xu, D. J. Hayes, W. Ren, S. Pan, D. N. Huntzinger, and S. C. Wofsy (2015), North American terrestrial CO2 uptake largely offset by CH4 and N2O emissions: toward a full accounting of the greenhouse gas budget, *Climatic change*, *129*(3-4), 413-426.

Tian, H., J. Yang, R. Xu, C. Lu, J. G. Canadell, E. A. Davidson, R. B. Jackson, A. Arneth, J. Chang, and P. Ciais (2019), Global soil nitrous oxide emissions since the preindustrial era estimated by an ensemble of terrestrial biosphere models: Magnitude, attribution, and uncertainty, *Global change biology*, *25*(2), 640-659.

Tian, H., R. Xu, J. G. Canadell, R. L. Thompson, W. Winiwarter, P. Suntharalingam, E. A. Davidson, P. Ciais, R. B. Jackson, and G. Janssens-Maenhout (2020), A comprehensive quantification of global nitrous oxide sources and sinks, *Nature*, *586*(7828), 248-256.

Tian, H., et al. (2018), The Global N2O Model Intercomparison Project, *Bulletin of the American Meteorological Society*, *99*(6), 1231-1251.

Usyskin-Tonne, A., Y. Hadar, U. Yermiyahu, and D. Minz (2020), Elevated CO2 has a significant impact on denitrifying bacterial community in wheat roots, *Soil Biology and Biochemistry*, *142*, 107697.

Virkkala, A. M., J. Aalto, B. M. Rogers, T. Tagesson, C. C. Treat, S. M. Natali, J. D. Watts, S. Potter, A. Lehtonen, and M. Mauritz (2021), Statistical upscaling of ecosystem CO2 fluxes across the terrestrial tundra and boreal domain: Regional patterns and uncertainties, *Global Change Biology*, *27*(17), 4040-4059.

Voigt, C., R. E. Lamprecht, M. E. Marushchak, S. E. Lind, A. Novakovskiy, M. Aurela, P. J. Martikainen, and C. Biasi (2017a), Warming of subarctic tundra increases emissions of all three important greenhouse gases–carbon dioxide, methane, and nitrous oxide, *Global Change Biology*, *23*(8), 3121-3138.

Voigt, C., M. E. Marushchak, R. E. Lamprecht, M. Jackowicz-Korczyński, A. Lindgren, M. Mastepanov, L. Granlund, T. R. Christensen, T. Tahvanainen, and P. J. Martikainen (2017b), Increased nitrous oxide emissions from Arctic peatlands after permafrost thaw, *Proceedings of the National Academy of Sciences*, *114*(24), 6238-6243.

Voigt, C., M. E. Marushchak, B. W. Abbott, C. Biasi, B. Elberling, S. D. Siciliano, O. Sonnentag, K. J. Stewart, Y. Yang, and P. J. Martikainen (2020), Nitrous oxide emissions from permafrost-affected soils, *Nature Reviews Earth & Environment*, *1*(8), 420-434.

Wagner-Riddle, C., K. A. Congreves, D. Abalos, A. A. Berg, S. E. Brown, J. T. Ambadan, X. Gao, and M. Tenuta (2017), Globally important nitrous oxide emissions from croplands induced by freeze–thaw cycles, *Nature Geoscience*, *10*(4), 279-283.

Walker, A. P., M. G. De Kauwe, A. Bastos, S. Belmecheri, K. Georgiou, R. F. Keeling, S. M. McMahon, B. E. Medlyn, D. J. P. Moore, and R. J. Norby (2021), Integrating the evidence for a terrestrial carbon sink caused by increasing atmospheric CO2, *New Phytologist*, *229*(5), 2413-2445.

Wang, X., S. Siciliano, B. Helgason, and A. Bedard-Haughn (2017), Responses of a mountain peatland to increasing temperature: A microcosm study of greenhouse gas emissions and microbial community dynamics, *Soil Biology and Biochemistry*, *110*, 22-33.

Watts, J. D., J. S. Kimball, L. A. Jones, R. Schroeder, and K. C. McDonald (2012), Satellite Microwave remote sensing of contrasting surface water inundation changes within the Arctic–Boreal Region, *Remote Sensing of Environment*, *127*, 223-236.

Wells, K. C., et al. (2018), Top-down constraints on global N2O emissions at optimal resolution: application of a new dimension reduction technique, *Atmos. Chem. Phys.*, *18*(2), 735-756.

Wilson, C., M. P. Chipperfield, M. Gloor, and F. Chevallier (2014), Development of a variational flux inversion system (INVICAT v1. 0) using the TOMCAT chemical transport model, *Geoscientific Model Development*, *7*, 2485-2500.

Yang, G., Y. Peng, M. E. Marushchak, Y. Chen, G. Wang, F. Li, D. Zhang, J. Wang, J. Yu, and L. Liu (2018), Magnitude and pathways of increased nitrous oxide emissions from uplands following permafrost thaw, *Environmental science & technology*, *52*(16), 9162-9169.

You, Y., and S. Pan (2020), Urban Vegetation Slows Down the Spread of Coronavirus Disease (COVID‐19) in the United States, *Geophysical Research Letters*, *47*(18), e2020GL089286.

Zaehle, S., P. Ciais, A. D. Friend, and V. Prieur (2011), Carbon benefits of anthropogenic reactive nitrogen offset by nitrous oxide emissions, *Nature Geoscience*, *4*(9), 601-605.

Soil nitrous oxide emissions across the northern high latitudes

Naiqing Pan[1], Hanqin Tian[1,2*], Hao Shi[3], Shufen Pan[4,1], Josep G. Canadell[5], Jinfeng Chang[6], Philippe Ciais[7], Eric A. Davidson[8], Gustaf Hugelius[9,10], Akihiko Ito[11], Robert B. Jackson[12], Fortunat Joos[13], Sebastian Lienert[13], Dylan B. Millet[14], Stefan Olin[15], Prabir K. Patra[16], Rona L. Thompson[17], Nicolas Vuichard[7], Kelley C. Wells[14], Chris Wilson[18,19], Yongfa You[1], Sönke Zaehle[20]

[1]Center for Earth System Science and Global Sustainability, Schiller Institute for Integrated Science and Society, Boston College, Chestnut Hill, MA, USA

[2]Department of Earth and Environmental Sciences, Boston College, Chestnut Hill, MA, USA

[3]State Key Laboratory of Urban and Regional Ecology, Research Center for Eco-Environmental Sciences, Chinese Academy of Sciences, Beijing, China

[4]Department of Engineering and Environmental Studies Program, Boston College, Chestnut Hill, MA, USA

5Global Carbon Project, CSIRO Oceans and Atmosphere, Canberra, Australian Capital Territory, Australia

[6] College of Environmental and Resource Sciences, Zhejiang University, Hangzhou, China

[7]Laboratoire des Sciences du Climat et de l'Environnement, LSCE, CEA CNRS, UVSQ UPSACLAY, Gif sur Yvette, France

[8]Appalachian Laboratory, University of Maryland Center for Environmental Science, Frostburg, MD, USA

[9]Department of Physical Geography, Stockholm University, Stockholm, Sweden

[10] Bolin Centre for Climate Research, Stockholm University, Stockholm, Sweden

[11] National Institute for Environmental Studies, Tsukuba, Japan

[12] Department of Earth System Science, Woods Institute for the Environment, Precourt Institute for Energy, Stanford University, Stanford, CA, USA

[13] Climate and Environmental Physics, Physics Institute and Oeschger Centre for Climate Change Research, University of Bern, Bern, Switzerland

[14] Department of Soil, Water, and Climate, University of Minnesota, St Paul, MN, USA

[15] Department of Physical Geography and Ecosystem Science, Lund University, Lund, Sweden

[16] Research Institute for Global Change, JAMSTEC, Yokohama, Japan

[17] Norsk Institutt for Luftforskning, NILU, Kjeller, Norway

[18] National Centre for Earth Observation, University of Leeds, Leeds, UK

[19] Institute for Climate and Atmospheric Science, School of Earth & Environment, University of Leeds, Leeds, UK

[20] Max Planck Institute for Biogeochemistry, Jena, Germany

*Corresponding author: Hanqin Tian (hanqin.tian@bc.edu)

Geophysical Research Letters (Submitted on January 18, 2024)

Abstract

Nitrous oxide (N_2O) is the most important stratospheric ozone-depleting agent based on current emissions and the third largest contributor to increased net radiative forcing. Increases in atmospheric N_2O have been attributed primarily to enhanced soil N_2O emissions. Critically, contributions from soils in the Northern High Latitudes (NHL, >50°N) remain poorly quantified despite their vulnerability to permafrost thawing induced by climate change. An ensemble of six terrestrial biosphere models suggests NHL soil N_2O emissions doubled since the preindustrial 1860s, increasing on average by 2.0±1.0 Gg N yr^{-1} (p<0.01). This trend reversed after the 1980s because of reduced nitrogen fertilizer application in non-permafrost regions and increased plant growth due to CO_2 fertilization suppressed emissions. However, permafrost soil N_2O emissions continued increasing attributable to climate warming; the interaction of climate warming and increasing CO_2 concentrations on nitrogen and carbon cycling will determine future trends in NHL soil N_2O emissions.

Key Points

1. N_2O emissions from northern high latitudes during 1997-2014 are estimated at 0.5–1.3 Tg N yr^{-1}, and soil was the largest source.

2. Northern high latitudes soil N_2O emissions increased from 0.3±0.1 Tg N yr^{-1} in 1861 to 0.6±0.3 Gg N yr^{-1} in 2016.

3. Climate change stimulated soil N_2O emissions, while the increased atmospheric CO_2 concentration suppressed emissions.

Plain Language Summary

Soils in the Northern High Latitudes (NHL) store large amounts of nitrogen, providing rich substrates for the emissions of nitrous oxide (N_2O) which is a potent greenhouse gas and ozone-depleting substance. The NHL has experienced rapid climate warming in recent decades, however, to what extent climate and other environmental factors have affected soil N cycling and N_2O emissions in the NHL remain poorly quantified. This study has provided the first quantification of the magnitudes and spatiotemporal variations of soil N_2O emissions across the NHL and showed that the NHL contributed about 8% of the increase in global soil N_2O emissions since pre-industrial period (the 1860s). Our results further reveal that changes in climate and atmospheric CO_2 concentration not only largely affected historical variations in soil N_2O emissions from the NHL but also will determine their future trends. Our study suggests the need to better understand climate and CO_2 controls on soil N_2O emissions and nitrogen cycling across the NHL and to improve their representation in earth system models.

1 Introduction

Nitrous oxide (N_2O) emissions have received increasing attention, because N_2O is the most important stratospheric ozone-depleting agent based on current emissions [*Ravishankara et al.*, 2009] and the third largest contributor to net radiative forcing by greenhouse gases [*Canadell et al.*, 2021; *Etminan et al.*, 2016]. The large amount of nitrogen additions to soils since the preindustrial period has significantly increased the atmospheric N_2O burden [*Canadell et al.*, 2021; *Tian et al.*, 2020]. Denitrification and nitrification are two primary soil processes controlling N_2O production, which are regulated by multiple factors such as temperature, water availability, acidity, substrate availability and microbial diversity [*Butterbach-Bahl et al.*, 2013; *Rees et al.*, 2013].

Over the past 40 years, the northern high latitudes, usually defined as the region north of 50°N [*Watts et al.*, 2012], have experienced climate warming at a rate faster than anywhere else on Earth [*Rantanen et al.*, 2022], a trend expected to continue in the coming decades [*Masson-Delmotte et al.*, 2021]. Therefore, there is an urgent need to understand and quantify how changes in climate and other environmental factors since the pre-industrial era have affected soil N_2O emissions from the NHL and thus have shaped the strength of climate-biogeochemical feedback.

The terrestrial nitrogen cycle in the NHL is closely related with permafrost, which underlays more than 60% of the area [*Brown et al.*, 1997]. Although large N stocks are stored in this region [*Harden et al.*, 2012; *Hugelius et al.*, 2020], the associated soil N_2O emissions have received little attention because they were considered to be small due to limited microbial activity and low mineralization rates under low-temperature and waterlogged conditions [*Voigt et al.*, 2020]. However, recent in-situ studies found that both barren and vegetated soils in the NHL can emit substantial amounts of N_2O [*Marushchak et al.*, 2011; *Marushchak et al.*, 2021; *Repo et al.*, 2009; *Voigt et al.*, 2017b]. Meanwhile, Arctic amplification, the phenomenon that climate change is amplified in the NHL, is projected to continue in the 21th century [*Christensen et al.*, 2013; *Pithan and Mauritsen*, 2014] with further implications for N_2O emissions: first, a large amount of immobile N stored in permafrost becomes available for decomposition and remobilization after permafrost thawing; second, rapid warming enhances N mineralization and promotes nitrification and denitrification; and third, warming may also promote biological nitrogen fixation (BNF), increasing ecosystem N availability and thereby potentially also N_2O production. Field experiments also confirm that warming can significantly increase N_2O emissions from permafrost-affected soils [*Cui et al.*, 2018; *Voigt et al.*, 2017b; *Wang et al.*, 2017].

Another influential factor for N_2O emissions in the NHL is the atmospheric CO_2 concentrations. Elevated atmospheric CO_2 concentrations do not have significant direct effects on reactive N flows controlling N_2O production, but can indirectly affect soil N_2O emissions by changing plant nitrogen uptake and root exudates due to enhanced plant growth [*Usyskin-Tonne et al.*, 2020]. On one hand, elevated atmospheric CO_2 promotes plant growth and thus more absorption of soil mineral N, restricting N_2O production [*Tian et al.*, 2019]. On the other hand, it may stimulate denitrification-derived N_2O emissions by increasing plant biomass and hence carbon substrate availability [*Kammann et al.*, 2008]. Additionally, elevated CO_2 can affect soil moisture by improving plant water-use efficiency, which can increase anaerobic conditions that stimulate denitrification [*Butterbach-Bahl et al.*, 2013]. Such contrasting effects of elevated CO_2 concentrations on N_2O emissions have been observed in field experiments [*Dijkstra et al.*, 2012; *Liu et al.*, 2018; *X Sun et al.*, 2018] but the magnitude of the CO_2 effect on northern soil N_2O emissions remains poorly understood.

Here, we investigated NHL soil N_2O emissions using six process-based terrestrial biosphere models (TBMs) from the global N_2O Model Intercomparison Project (NMIP) [*Tian et al.*, 2018]. Using factorial simulation experiments, we quantified the contributions of different driving factors, particularly climate change and rising atmospheric CO_2, to the variations in soil N_2O emissions during 1861-2016. Statistical methods were further employed to disentangle the effects of temperature and precipitation on soil N_2O emissions. We also compared bottom-up (BU, including process-based TBMs for soil emissions and emission factor approaches for non-soil emissions) estimates of N_2O emissions with those of three atmospheric inversion frameworks (top-down, TD) [*Rona L. Thompson et al.*, 2019] to investigate the uncertainties in current estimates of N_2O emissions from the NHL.

2 Materials and methods

2.1 Data sources

2.1.1 Soil N_2O emissions

An ensemble estimate of soil N_2O emissions from the NHL was derived from simulations by the six TBMs that participated in the NMIP: (1) DLEM [*Tian et al.*, 2015], (2) LPJ-GUESS [*Olin et al.*, 2015], (3) LPX-Bern [*Joos et al.*, 2020], (4) O-CN [*Zaehle et al.*, 2011], (5) ORCHIDEE-CNP [*Goll et al.*, 2017; *Y Sun et al.*, 2021], and (6) VISIT [*Inatomi et al.*, 2010]. Each model performed a subset of seven simulations (S0-S6) to quantify N_2O emissions from both agricultural and natural soils, and to disentangle the effects of multiple environmental factors on N_2O emissions (Table S1). The differences between pairs of simulations, i.e. S1-S2, S2-S3, S3-S4, S4-S5, S5-S6, and S6-S0, were used to evaluate the effects of manure N, mineral N fertilizer, atmospheric N deposition, land use and land cover change (LULCC), atmospheric CO_2 concentration, and climate, respectively. More information about the model simulation protocol and forcing data can refer to *Tian et al.* [2018]. Among the six NMIP models, LPJ-GUESS and LPX-Bern have dedicated permafrost modules and consider freeze-thaw processes; O-CN lacks an explicit permafrost representation but describes freeze-thaw cycles; the other models have no explicit representation of the permafrost layer or freeze-thaw processes.

2.1.2 Fire-induced N_2O emissions and non-soil anthropogenic N_2O emissions

N_2O emissions from biomass burning were from the GFED4.1s dataset. N_2O emissions from non-soil anthropogenic sources were obtained from EDGAR 6.0 [*Crippa et al.*, 2019]. EDGAR non-soil anthropogenic emissions were combined with GFED biomass burning emissions and with

NMIP soil emissions to constitute BU estimates of total N_2O emissions, aiming to make comparison with TD estimates.

2.1.3 Top-down N_2O emission estimates

Three independent atmospheric inversion models were used: GEOS-Chem [*Wells et al.*, 2018], INVICAT [*Wilson et al.*, 2014] and MIROC4-ACTM [*Patra et al.*, 2018; *Patra et al.*, 2022]. GEOS-Chem and INVICAT used the same prior estimates: soil emissions from the O-CN model, biomass burning emissions from GFEDv4.1s, and non-soil anthropogenic emissions from EDGAR v4.2FT2010. The MIROC4-ACTM prior used natural soil emissions from the VISIT model, and all anthropogenic emissions from EDGAR 4.2. The MIROC4-ACTM prior included agricultural burning but did not explicitly include wildfire emissions. All models used the Bayesian inversion framework to find the optimal emissions that provide the best agreement to observed N_2O mixing ratios while being coupled to an atmospheric transport model.

2.2 Statistical methods

The path analysis model (PAM) was used to investigate how climatic factors affected permafrost soil N_2O emissions. PAM can deal with complex relationships among multiple independent and dependent variables, and disentangle direct and indirect effects of the explanatory variables on the response variable [*Alwin and Hauser*, 1975; *You and Pan*, 2020]. Here, we developed the conceptual model by specifying the relationships between climatic factors and soil N_2O emissions and considering the interactions between these factors. We also conducted partial correlation analysis between soil N_2O emissions and temperature/precipitation. The temporal sensitivities of soil N_2O emissions to temperature and precipitation were fitted using a multiple regression model. The Mann–Kendall test was used to assess the significance of trends in N_2O emissions.

3 Results

3.1 Spatiotemporal variations of soil N_2O emissions since the 1860s

Multi-model ensemble estimates show that soil N_2O emissions from the NHL increased from 312±125 Gg N yr^{-1} in 1861 to 605±269 Gg N yr^{-1} in 2016 (Fig.1a), with an average increase rate of 2.0±1.0 Gg N yr^{-1} (p<0.01). Soil N_2O emissions from non-permafrost regions dominated the temporal variations of total NHL emissions, which were relatively stable over the first five decades, then rapidly increased from the 1920s to the 1980s, and peaked in the 1980s. In the late 1980s and early 1990s, northern soil N_2O emissions drastically decreased and fluctuated afterwards. Meanwhile, soil N_2O emissions from permafrost regions showed different temporal dynamics; they remained relatively stable before the 1980s, and rapidly increased thereafter. In the 1860s, the highest emission density occurred in Central Europe. During 1861-2016, soil N_2O emissions from most regions significantly increased. In the recent decade (2007-2016), Western Europe had the highest emission density (Fig.1b-d), and more than half of the soil N_2O emissions were from croplands (Fig. S2). During 1861-1980, the fastest increase in N_2O emissions occurred in Western and Central Europe where the average increase exceeded 2×10^{-4} g N m^{-2} yr^{-1} (Fig.1e). However, trends in soil N_2O emissions have largely changed since 1980, with emissions significantly decreasing in Eastern Europe and Russia but rapidly increasing in Siberia and Southern Canada (Fig.1f).

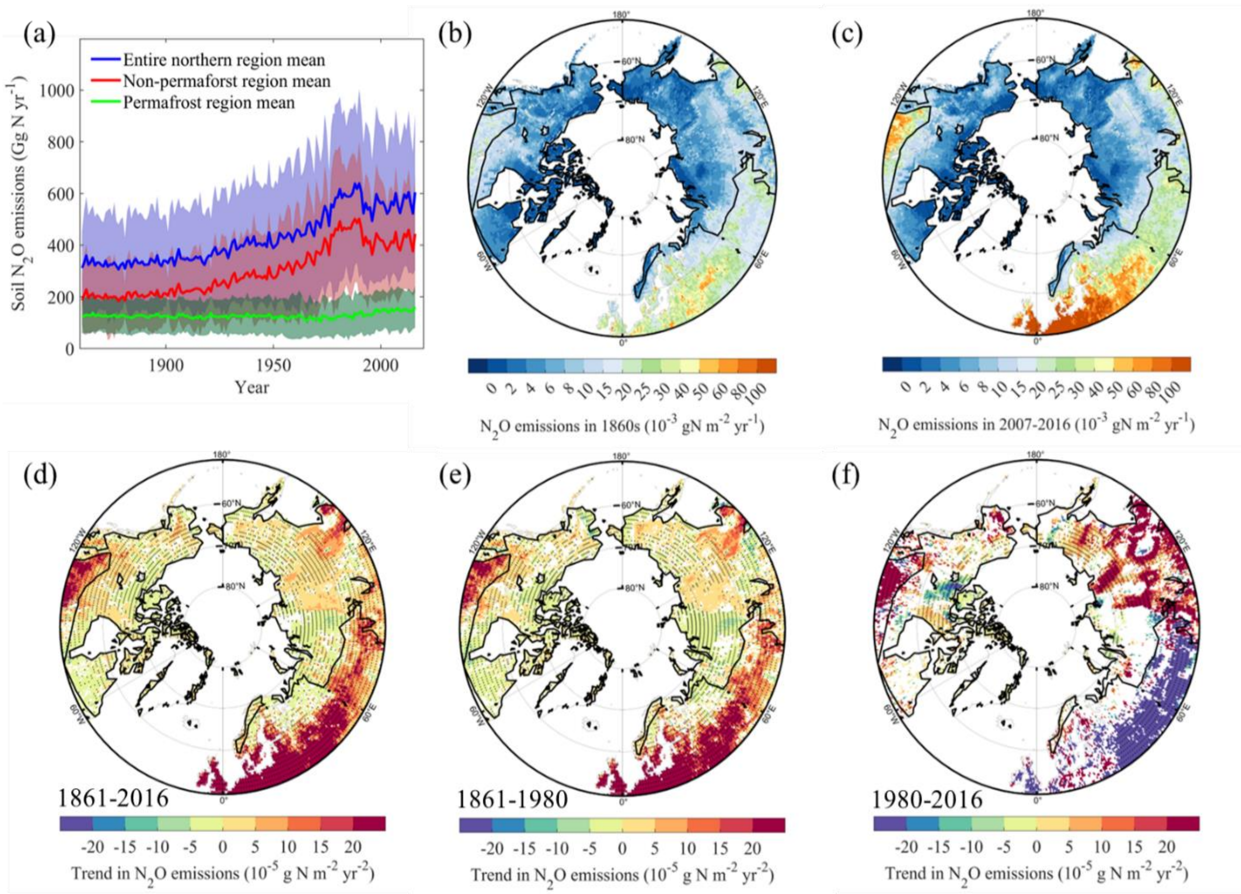

Fig. 1: (a) Changes in soil N_2O emissions from the NHL, the shaded area indicates one standard deviation of all estimates. (b) and (c) show spatial pattern of mean annual soil N_2O emissions during the 1860s and 2007-2016, respectively. Trends in soil N_2O emissions during 1861-2016 (d), 1861-1980 (e), and 1980-2016 (f); grids with non-significant trends ($p>=0.05$) were excluded, and stippling indicates where a majority of models (at least 4 out of 6) agree on the sign of the trend.

3.2 Contributions of different driving factors to soil N_2O emissions during 1861-2016

Our results derived from factorial simulations suggested that increasing atmospheric CO_2 concentrations reduced NHL soil N_2O emissions, while the other five factors stimulated N_2O emissions (Fig. 2a). Climate change played a dominant role in stimulating N_2O emissions before the 1930s and N inputs made increasing contributions from the 1940s to the 1980s. From the 1860s to the 1980s, fertilizer application contributed 53% to the increase in emissions, followed by atmospheric N deposition (26%), manure N application (15%), climate change (12%), and land use change (5%). The effect of increased atmospheric CO_2 (-10%) almost offset that of climate change. Since the 1980s, the role of anthropogenic N inputs in stimulating N_2O emissions weakened gradually; by contrast, drastic warming and wetting made climate change increasingly important (Fig. S3). Over the entire study period, climate change made the second largest contribution (37%) to the increase of NHL soil emissions after N fertilizer application (42%). Climate change had a larger relative contribution to the emission increase in permafrost regions (Fig. 2c) than in non-permafrost regions. During 1861-2016, climate change contributed 114% (partly offset by the negative CO_2 effect) to the emission increase in permafrost regions, which was stronger than in non-permafrost regions (28%) (Fig. 2d). All individual models agreed that climate change made a larger relative contribution to emission increases in permafrost regions than in non-permafrost regions, and that the effects of climate change have increased since the 1980s (Fig. S4-6). In most northern regions, trends in soil N_2O emissions were dominated by climate change; fertilizer only dominated trends in Western Europe and some intensive agricultural lands over Eastern Europe, Russia, and south Canada, while atmospheric N deposition dominated trends in part of Central and Eastern Europe. Regions dominated by other factors were relatively small (Fig. 2b).

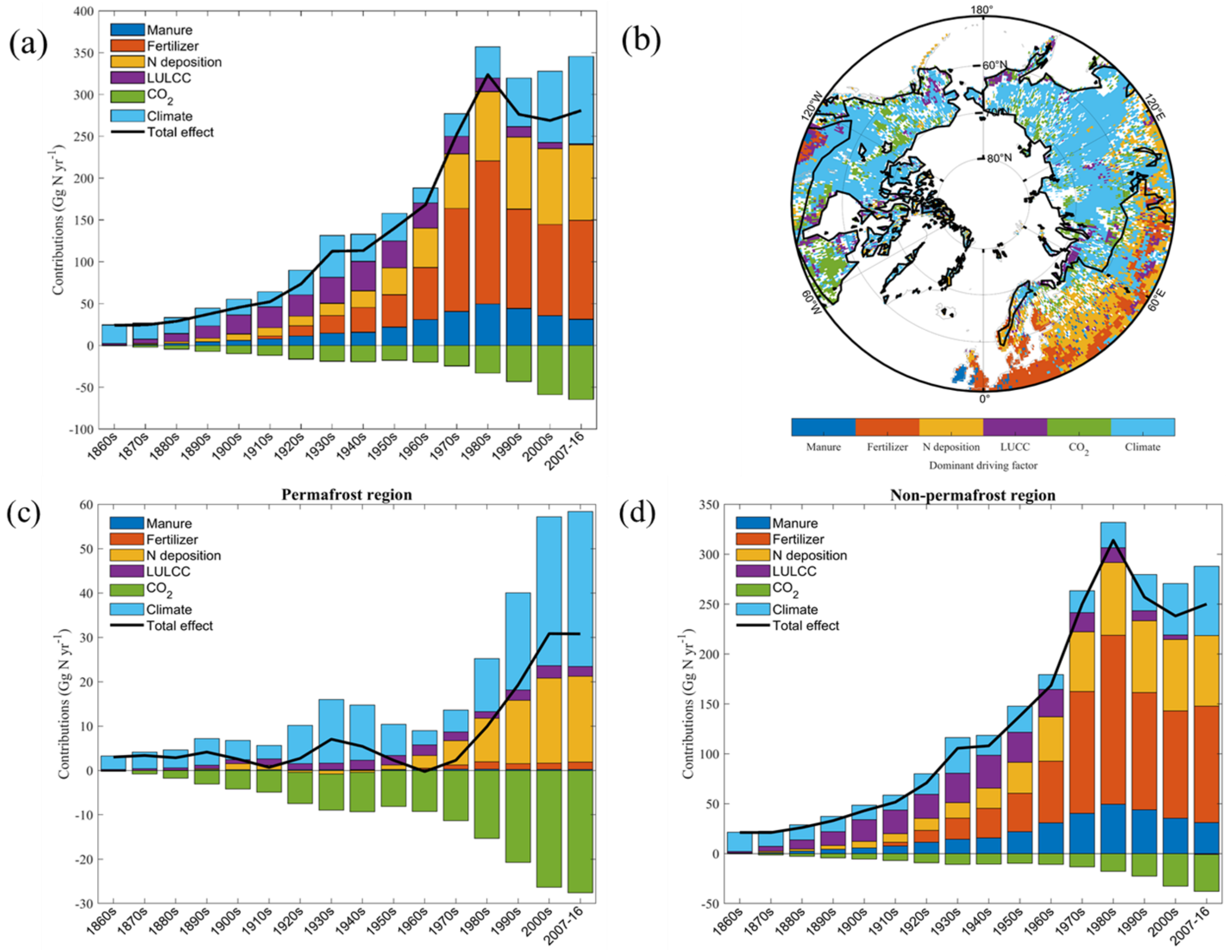

Fig. 2: (a) Decadal variations in the contributions of different driving factors. (b) Distribution of dominant driving factors of soil N_2O emissions during 1861-2016; grids with non-significant trends were excluded. Contributions of different driving factors to soil N_2O emissions from permafrost regions (c) and non-permafrost regions (d).

3.3 Effects of temperature and precipitation on soil N_2O emissions

Temperature and precipitation changes alter soil microclimate , nutrient availability and microbial ecology , thereby influencing N_2O emissions [*Dalal and Allen*, 2008]. For the entire NHL, both temperature and precipitation significantly increased during 1901-2016, with rates of 0.14 ℃ per decade and 0.38 mm yr^{-1} (10% total increase since the 1900s), respectively (Fig. S3). According to multiple regression model results, the sensitivities of soil N_2O emissions to temperature and precipitation were 29±21 Gg N °C^{-1} and 0.4±0.7 Gg N mm^{-1} during 1901-2016, suggesting that warming and wetting increased soil N_2O emissions by 48±35 Gg N yr^{-1} and 15±26 Gg N yr^{-1}, respectively. The path analysis model also suggested that warming contributed more to soil N_2O emission increases than wetting (Fig. S7). Both warming and wetting have accelerated since 1980 (Fig. S3, S8, S9), with average rates of 0.38 °C per decade and 0.57 mm yr^{-2}, respectively. At the same time, the sensitivities of soil N_2O emissions to temperature and precipitation increased to 38±22 Gg N °C^{-1} and 1.2±0.8 Gg N mm^{-1}, respectively. These two factors together led to the large climate effects in the recent four decades.

Soil N_2O emissions were positively correlated with temperature in most northern regions (Fig. S10a). Compared with the 1901-1980 period, warming after 1980 was more pronounced and prevalent (Fig. S8-9), which enhanced biological N fixation and net N mineralization and further promoted nitrification and denitrification (Fig. S11). During the study period, most of the NHL experienced significant warming (Fig. S10c), indicating that warming universally stimulated N_2O emissions in this region. Recent manipulation experiments also suggest that warming can significantly increase soil N_2O emissions from the NHL [*Cui et al.*, 2018; *Voigt et al.*, 2017b; *Wang et al.*, 2017]. Unlike temperature, the correlation between soil N_2O emissions and precipitation varied spatially (Fig. S10b). Although a large area of the NHL experienced significant wetting (Fig. S10d), the positive effects of wetting on emissions from Eastern Europe, central Canada and Siberia were partly counteracted by the negative effects in Northern Europe and northwestern Russia, which explained why precipitation had a smaller effect than temperature on the regional total emissions.

3.4 Declining soil N_2O emissions since the 1980s

Soil N_2O emissions from the NHL rapidly increased before the 1980s, however, declined thereafter. Although total BNF over the NHL increased since 1980 (Fig. S12), the ensemble mean of soil N_2O emissions from the NHL decreased at an average rate of -1.1 GgN yr^{-1} ($p<0.05$) during 1980-2016 (Fig. 3a). The rapid decline in emissions during 1988-1996 was due to reduced fertilizer application, after which period the negative effect of CO_2 fertilization was enhanced (Fig. S14). The most pronounced decline occurred in Eastern Europe and Russia (Fig. 1f), mainly caused by the sharp decrease in external nitrogen inputs due to the collapse of the Soviet Union (Fig. S14). Concurrently, soil emissions from Siberia and Southern Canada significantly increased, due to climate change and nitrogen enrichment, respectively (Fig. S14). Soil N_2O emissions fluctuated after 1998 because the positive climate effect was counteracted by combined effects of fertilizer application, CO_2 and land use change.

The dominant drivers of negative effects differed between permafrost and non-permafrost regions. In permafrost regions, elevated CO_2 concentration was the only factor suppressing soil N_2O emissions and counteracted more than half of the climate-induced emissions (Fig. 3b). By contrast, reduced N fertilizer application, elevated CO_2 concentration and land use change jointly reduced emissions from non-permafrost regions (Fig. 3c). For the entire NHL, the atmospheric CO_2-induced decline in soil N_2O emissions surpassed the effect of reduced fertilizer application over the recent decade. Elevated atmospheric CO_2 significantly suppressed N_2O emissions in most northern regions (Fig. S14). Since the 1980s, increased atmospheric CO_2 concentrations stimulated terrestrial gross primary production (Fig. S15a, c), thus enhancing plant nitrogen uptake (Fig. S15b, d) and reducing the availability of soil inorganic nitrogen, which finally suppressed N_2O emissions.

The largest stimulation effect of CO_2 on vegetation growth and nitrogen uptake occurred in the boreal forests, where the CO_2-induced suppression of N_2O emissions was the most pronounced. Enhanced vegetation growth in the NHL has been reported in previous studies [*Berner et al.*, 2020; *Myers-Smith et al.*, 2020; *Virkkala et al.*, 2021]. Reduced N_2O emissions due to enhanced plant growth and nitrogen uptake is also consistent with field observations in the NHL [*Gong and Wu*, 2021; *Marushchak et al.*, 2011; *Stewart et al.*, 2012].

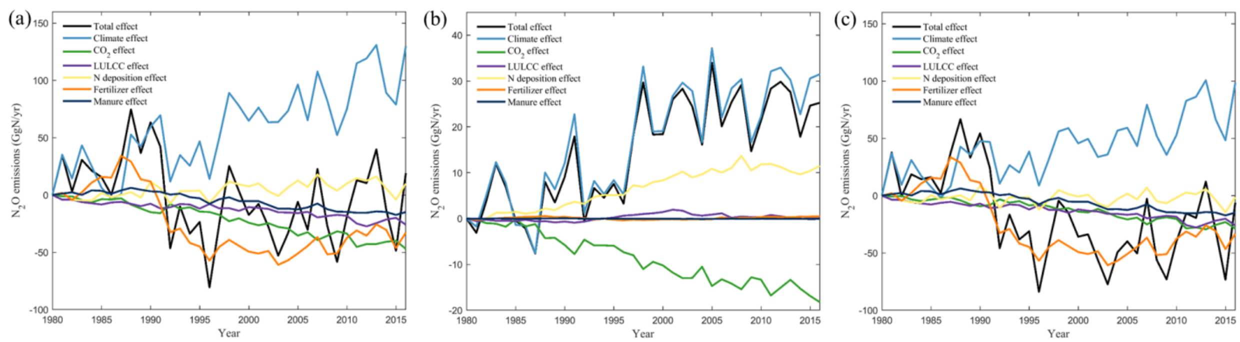

Fig. 3: Contributions of different driving factors in the entire NHL (a), permafrost regions (b), and non-permafrost regions (c) during 1980-2016.

3.5 Comparison with TD estimates

Using the current N_2O observation network, TD models estimate total N_2O emissions with its spatial distribution across the land but cannot well quantify the contributions of different sources. With the aim of comparing BU estimates with TD estimates, we added N_2O emissions from soil, biomass burning and non-soil anthropogenic sources (Fig. S16) together to constitute BU estimates of total N_2O emissions. According to the resulting BU estimates, soil was the largest source of N_2O emissions in the NHL (mean value: 572 Gg N yr^{-1} during 1998-2014), followed by non-soil anthropogenic sources (280 Gg N yr^{-1}) and biomass burning (143 Gg N yr^{-1}). Both BU and TD approaches indicated similar spatial emission patterns (Fig. 4), but the ensemble mean of total BU estimate (995±267 Gg N yr^{-1}) was substantially higher than the TD estimate (668±134 Gg N yr^{-1}) for the overlapping 1998-2014 period. Both TD and BU approaches revealed that the total N_2O emissions had no significant trend during this period (p>0.05). Removing N_2O emitted by biomass burning and non-soil anthropogenic sources from the TD estimates, the remaining N_2O exhibited a decreasing trend during 1998-2014 (from -10.0 to -3.2 Gg N yr^{-2}, mean -7.3 Gg N yr^{-2}), implying that the TD models also suggest a decreasing trend in NHL soil N_2O emissions.

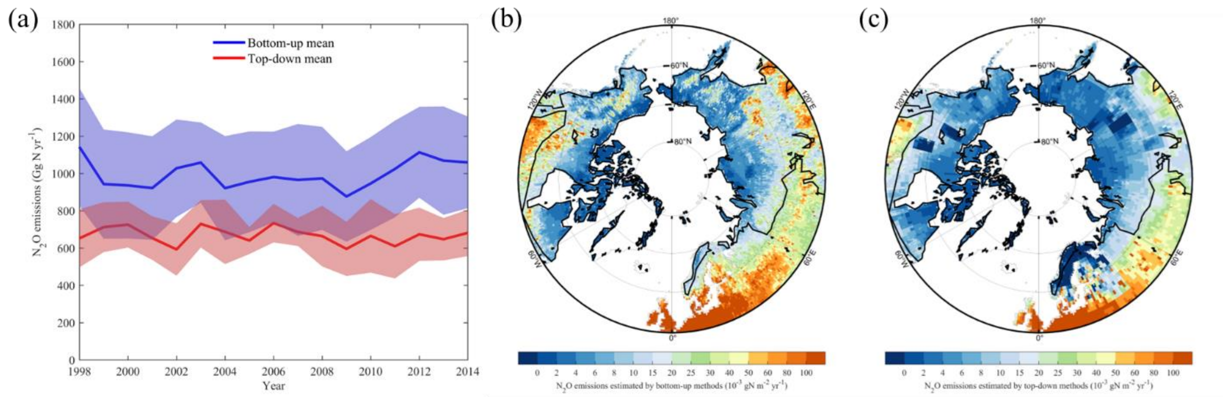

Fig. 4: (a) Comparison between TD and BU estimates of total N_2O emissions, the lines represent the ensemble means and the shaded areas indicate one standard deviation of model estimates. Spatial pattern of total N_2O emissions estimated by BU (b) and TD (c) approaches.

3.6 Comparison with empirical estimates

Based on site-level observation data, *Voigt et al.* [2020] estimated soil N_2O emissions from permafrost regions using a simple extrapolation method, and proposed that peatlands had the highest N_2O emissions among natural permafrost ecosystems. However, these extrapolation-based estimates have large uncertainties, with the implied annual soil N_2O emissions from the NHL ranging from 140 to 1030 Gg N^{-1}. In particular, estimates based on mean fluxes are an order of magnitude larger than those based on median fluxes because of several N_2O emission hot spots. Combining observed peatland annual fluxes and peatland distribution maps, *Hugelius et al.* [2020] estimated a much smaller northern peatland source of 22 ± 5 Gg $N \cdot y^{-1}$, with only half of that peatland area being permafrost. This suggests a smaller source than the estimates of *Voigt et al.* [2020]. NMIP estimates of soil N_2O emissions from the permafrost regions are close to the lower-limit of estimates by *Voigt et al.* [2020], and have smaller uncertainty range (0.11-0.26 Tg N^{-1}, mean 0.17 Tg N^{-1}), which partly reflect the usage of unified model input data. Soil N_2O emissions from non-permafrost regions are largely controlled by fertilizer and manure applications. According to NMIP models, the average emission factors of fertilizer and manure in non-permafrost regions during 1980-2016 were 1.4% and 1.7%, respectively. Both factors were positively correlated with temperature and precipitation, suggesting positive interactions between nitrogen additions and climate change [*Tian et al.*, 2020].

4 Discussion

Our study provides a first estimate of soil N_2O emissions from the NHL, although large uncertainties remain in both TD and BU approaches (Fig. S17, S18). Since the process-based models used in this study were driven by the same input data, differences were mainly induced by missing or uncertain representation of important processes such as seasonal freeze-thaw cycles and permafrost thaw [*Risk et al.*, 2013], BNF [*Meyerholt et al.*, 2020] and reactive N flows through ecosystems [*Butterbach-Bahl et al.*, 2013], and critical information such as timing and frequency of fertilizer application [*Nishina et al.*, 2017]. Several NMIP models do not include an explicit permafrost layer or freeze-thaw processes; inclusion of such factors would enable better representation of "hot spots" and "hot moments" soil N_2O emissions in the NHL [*Voigt et al.*, 2020;

Wagner-Riddle et al., 2017]. Current process-based TBMs also have insufficient representation of the upland thermokarst formation [*Yang et al.*, 2018] and fine-grained landscape structure of arctic ecosystems (e.g., landscape elements that are ultra-emitters of N_2O such as non-vegetated organic soil). Integrating sub-grid scale information and processes into models may provide a solution for fine-grained physical-hydrological modelling. As revealed by *Voigt et al.* [2020], peatlands have the highest N_2O emission rate in permafrost regions. It is thus important for process-based TBMs to explicitly consider peatland thermal, hydrological, and biogeochemical processes.

TD estimates have a stronger dependence on the prior fluxes in NHL where atmospheric N_2O measurements are sparse [*Nevison et al.*, 2018; *Rona Louise Thompson et al.*, 2014; *Rona L. Thompson et al.*, 2019]. In this study, the average prior N_2O flux employed in the TD models (846±141 Gg N yr^{-1}) was lower than our BU estimates (955±267 Gg N yr^{-1}). These low prior N_2O fluxes, as well as lower TD emissions in summer compared to the BU estimates, are the likely causes of the lower TD estimates (Fig. S18). Differing prior N_2O fluxes between the inversions (see methods) also lead to somewhat varying inversion estimates. Using the ensemble mean NMIP soil emission estimates as prior for the TD inversions may improve model agreement. The total prior ocean flux also has important impacts on the magnitude of the terrestrial flux. However, there have been few observational constraints on the ocean source until recently [*Patra et al.*, 2022]. The sparseness of atmospheric observations over both land and ocean north of 50°N and systematic model errors in stratosphere-troposphere exchange increase the uncertainty in TD estimates. Building denser regional N_2O monitoring networks and launching (regular) aircraft campaigns in the NHL will help better constrain inversion models [*Bisht et al.*, 2021].

Our results suggest that the NHL contributed approximately 8% of the increase in global soil N_2O emissions during 1861-2016 [*Tian et al.*, 2019]. Warming and wetting stimulated NHL soil N_2O emissions, while elevated CO_2 concentrations suppressed emissions (through increased plant growth and larger uptake of soil N), findings that are in line with field observations [*Cui et al.*, 2018; *Dijkstra et al.*, 2012; *Gong and Wu*, 2021; *Marushchak et al.*, 2011; *Voigt et al.*, 2017a]. From 1980-2016 when warming was strongest, the NHL contributed 14% of global climate effect enhancing soil N_2O emissions. Under the SSP370 and SSP585 scenarios, CMIP6 climate models predict that the mean temperature of the NHL will increase by 6.2 (4.1-9.8) ℃ and 7.8 (5.5-12.1) ℃, respectively, during 2015-2100; the mean precipitation will increase by 96（65-177）mm yr^{-1} and 129（51-206）mm yr^{-1}, respectively (Fig. S19). If the sensitivities of soil N_2O emissions to temperature and precipitation in the future are consistent with historical values, future climate change alone will substantially increase NHL soil N_2O emissions. However, atmospheric CO_2 concentrations also rapidly increase under SSP370 and SSP585 scenarios (Fig. S20), potentially offsetting a significant fraction of the positive climate effect if arctic vegetation continues to take up more carbon and nitrogen with elevated CO_2. Uncertainties arise regarding the degree of recycling of that extra nitrogen uptake in soils by mineralization. The magnitude of the future CO_2 effect is also highly uncertain [*Walker et al.*, 2021], and how it will affect future northern N_2O emissions requires further study. Reconstructions from ice cores show that global N_2O emissions increased over the last deglaciation when the climate warmed, CO_2 increased, and land carbon inventories grew in size, providing evidence for a net positive relationship between past warming, CO_2, land carbon, stocks, and N_2O emissions at the global scale [*Fischer et al.*, 2019; *Joos et al.*, 2020].

Since the NMIP project did not design simulation experiments to separate the effects of temperature and precipitation on soil N_2O emissions, we used statistical methods to explore these relationships. However, the collinearity between temperature and precipitation variations may undermine the reliability of the inferred sensitivities of soil N_2O emissions to temperature and precipitation. Future model intercomparison projects need to design simulations to disentangle the effects of temperature and precipitation.

Acknowledgements

This study was resulted from NMIP (global N/N2O Model Intercomparison Project) co-sponsored by Global Carbon Project and International Nitrogen Initiative. This work contributes to the REgional Carbon Cycle Assessment and Porcesses-2 of the Global Carbon Project. H.T., N. Pan, S. Pan acknowledge funding support from NSF (grant nos. 1903722, 1922687); PKP is partly funded by the Arctic Challenge for Sustainability phase II (ArCS-II; JPMXD1420318865) Projects of the Ministry of Education, Culture, Sports, Science and Technology (MEXT); KCW and DBM acknowledge support from NASA (Grant #NNX17AK18G) and NOAA (Grant #NA13OAR4310086).

Data availability statement

EDGAR 6.0 dataset is available at https://edgar.jrc.ec.europa.eu/dataset_ghg60. GFED4.1s dataset is available at https://www.geo.vu.nl/~gwerf/GFED/GFED4/. Soil N_2O emissions, terrestrial GPP and plant nitrogen uptake estimated by NMIP models and top-down N_2O emission are available at https://datadryad.org/stash/share/isclqpURaZ5GJLLok3LCvjBrQ20ybXX7M3dQzuVWFCk

Author contributions

H.T. initiated and designed this research, N.P. conducted data analysis and synthesis, N.P. and H.T. drafted the manuscript. All co-authors contributed to the writing and development of the manuscript.

Competing interests

The authors declare no competing interests.

References

Alwin, D. F., and R. M. Hauser (1975), The decomposition of effects in path analysis, *American sociological review*, 37-47.

Berner, L. T., R. Massey, P. Jantz, B. C. Forbes, M. Macias-Fauria, I. Myers-Smith, T. Kumpula, G. Gauthier, L. Andreu-Hayles, and B. V. Gaglioti (2020), Summer warming explains widespread but not uniform greening in the Arctic tundra biome, *Nature communications*, *11*(1), 1-12.

Bisht, J. S. H., T. Machida, N. Chandra, K. Tsuboi, P. K. Patra, T. Umezawa, Y. Niwa, Y. Sawa, S. Morimoto, and T. Nakazawa (2021), Seasonal Variations of SF6, CO2, CH4, and N2O in the UT/LS Region due to Emissions, Transport, and Chemistry, *Journal of Geophysical Research: Atmospheres*, *126*(4), e2020JD033541.

Brown, J., O. J. Ferrians Jr, J. A. Heginbottom, and E. S. Melnikov (1997), Circum-arctic map of permafrost and ground ice conditions.

Butterbach-Bahl, K., L. Baggs, M. Dannenmann, R. Kiese, and S. Zechmeister-Boltenstern (2013), Nitrous oxide emissions from soils: How well do we understand the processes and their controls?, *Philosophical transactions of the Royal Society of London. Series B, Biological sciences*, *368*, 20130122.

Canadell, J. G., P. M. S. Monteiro, M. H. Costa, L. C. Da Cunha, P. M. Cox, V. Alexey, S. Henson, M. Ishii, S. Jaccard, and C. Koven (2021), Global carbon and other biogeochemical cycles and feedbacks, edited.

Christensen, J. H., K. K. Kanikicharla, E. Aldrian, S. I. An, I. F. A. Cavalcanti, M. de Castro, W. Dong, P. Goswami, A. Hall, and J. K. Kanyanga (2013), Climate phenomena and their relevance for future regional climate change, in *Climate change 2013 the physical science basis: Working group I contribution to the fifth assessment report of the intergovernmental panel on climate change*, edited, pp. 1217-1308, Cambridge University Press.

Crippa, M., G. Oreggioni, D. Guizzardi, M. Muntean, E. Schaaf, E. Lo Vullo, E. Solazzo, F. Monforti-Ferrario, J. G. J. Olivier, and E. Vignati (2019), Fossil CO2 and GHG emissions of all world countries, *Publication Office of the European Union: Luxemburg*.

Cui, Q., C. Song, X. Wang, F. Shi, X. Yu, and W. Tan (2018), Effects of warming on N2O fluxes in a boreal peatland of Permafrost region, Northeast China, *Science of The Total Environment*, *616-617*, 427-434.

Dalal, R. C., and D. E. Allen (2008), Greenhouse gas fluxes from natural ecosystems, *Australian Journal of Botany*, *56*(5), 369-407.

Dijkstra, F. A., S. A. Prior, G. B. Runion, H. A. Torbert, H. Tian, C. Lu, and R. T. Venterea (2012), Effects of elevated carbon dioxide and increased temperature on methane and nitrous oxide fluxes: evidence from field experiments, *Frontiers in Ecology and the Environment*, *10*(10), 520-527.

Etminan, M., G. Myhre, E. J. Highwood, and K. P. Shine (2016), Radiative forcing of carbon dioxide, methane, and nitrous oxide: A significant revision of the methane radiative forcing, *Geophysical Research Letters*, *43*(24), 12-614.

Fischer, H., et al. (2019), N2O changes from the Last Glacial Maximum to the preindustrial – Part 1: Quantitative reconstruction of terrestrial and marine emissions using N2O stable isotopes in ice cores, *Biogeosciences*, *16*(20), 3997-4021.

Goll, D. S., et al. (2017), A representation of the phosphorus cycle for ORCHIDEE (revision 4520), *Geosci. Model Dev.*, *10*(10), 3745-3770.

Gong, Y., and J. Wu (2021), Vegetation composition modulates the interaction of climate warming and elevated nitrogen deposition on nitrous oxide flux in a boreal peatland, *Global Change Biology*, *27*(21), 5588-5598.

Harden, J. W., et al. (2012), Field information links permafrost carbon to physical vulnerabilities of thawing, *Geophysical Research Letters*, *39*(15).

Hugelius, G., J. Loisel, S. Chadburn, R. B. Jackson, M. Jones, G. MacDonald, M. Marushchak, D. Olefeldt, M. Packalen, and M. B. Siewert (2020), Large stocks of peatland carbon and nitrogen are vulnerable to permafrost thaw, *Proceedings of the National Academy of Sciences*, *117*(34), 20438-20446.

Inatomi, M., A. Ito, K. Ishijima, and S. Murayama (2010), Greenhouse gas budget of a cool-temperate deciduous broad-leaved forest in Japan estimated using a process-based model, *Ecosystems*, *13*(3), 472-483.

Joos, F., R. Spahni, B. D. Stocker, S. Lienert, J. Müller, H. Fischer, J. Schmitt, I. C. Prentice, B. Otto-Bliesner, and Z. Liu (2020), N_2O changes from the Last Glacial Maximum to the preindustrial – Part 2: terrestrial N_2O emissions and carbon–nitrogen cycle interactions, *Biogeosciences*, *17*(13), 3511-3543.

Kammann, C., C. Müller, L. Grünhage, and H.-J. Jäger (2008), Elevated CO2 stimulates N2O emissions in permanent grassland, *Soil Biology and Biochemistry*, *40*(9), 2194-2205.

Liu, S., C. Ji, C. Wang, J. Chen, Y. Jin, Z. Zou, S. Li, S. Niu, and J. Zou (2018), Climatic role of terrestrial ecosystem under elevated CO 2: a bottom ‐ up greenhouse gases budget, *Ecology letters*, *21*(7), 1108-1118.

Marushchak, M. E., A. PitkÄMÄKi, H. Koponen, C. Biasi, M. SeppÄLÄ, and P. J. Martikainen (2011), Hot spots for nitrous oxide emissions found in different types of permafrost peatlands, *Global Change Biology*, *17*(8), 2601-2614.

Marushchak, M. E., J. Kerttula, K. Diáková, A. Faguet, J. Gil, G. Grosse, C. Knoblauch, N. Lashchinskiy, P. J. Martikainen, and A. Morgenstern (2021), Thawing Yedoma permafrost is a neglected nitrous oxide source, *Nature communications*, *12*(1), 1-10.

Masson-Delmotte, V., P. Zhai, A. Pirani, S. L. Connors, C. Péan, S. Berger, N. Caud, Y. Chen, L. Goldfarb, and M. I. Gomis (2021), Climate Change 2021: The Physical Science Basis. Contribution of Working Group I to the Sixth Assessment Report of the Intergovernmental Panel on Climate Change, *IPCC: Geneva, Switzerland*.

Meyerholt, J., K. Sickel, and S. Zaehle (2020), Ensemble projections elucidate effects of uncertainty in terrestrial nitrogen limitation on future carbon uptake, *Global Change Biology*, *26*(7), 3978-3996.

Myers-Smith, I. H., J. T. Kerby, G. K. Phoenix, J. W. Bjerke, H. E. Epstein, J. J. Assmann, C. John, L. Andreu-Hayles, S. Angers-Blondin, and P. S. Beck (2020), Complexity revealed in the greening of the Arctic, *Nature Climate Change*, *10*(2), 106-117.

Nevison, C., A. Andrews, K. Thoning, E. Dlugokencky, C. Sweeney, S. Miller, E. Saikawa, J. Benmergui, M. Fischer, and M. Mountain (2018), Nitrous oxide emissions estimated with the CarbonTracker ‐ Lagrange North American regional inversion framework, *Global Biogeochemical Cycles*, *32*(3), 463-485.

Nishina, K., A. Ito, N. Hanasaki, and S. Hayashi (2017), Reconstruction of spatially detailed global map of NH4+ and NO3− application in synthetic nitrogen fertilizer, *Earth Syst. Sci. Data*, *9*(1), 149-162.

Olin, S., M. Lindeskog, T. A. M. Pugh, G. Schurgers, D. Wårlind, M. Mishurov, S. Zaehle, B. D. Stocker, B. Smith, and A. Arneth (2015), Soil carbon management in large-scale Earth system modelling: implications for crop yields and nitrogen leaching, *Earth System Dynamics*, *6*(2), 745-768.

Patra, P. K., M. Takigawa, S. Watanabe, N. Chandra, K. Ishijima, and Y. Yamashita (2018), Improved chemical tracer simulation by MIROC4. 0-based atmospheric chemistry-transport model (MIROC4-ACTM), *Sola*, *14*, 91-96.

Patra, P. K., E. J. Dlugokencky, J. W. Elkins, G. S. Dutton, Y. Tohjima, M. Sasakawa, A. Ito, R. F. Weiss, M. Manizza, and P. B. Krummel (2022), Forward and inverse modelling of atmospheric nitrous oxide using MIROC4-atmospheric chemistry-transport model, *Journal of the Meteorological Society of Japan. Ser. II*.

Pithan, F., and T. Mauritsen (2014), Arctic amplification dominated by temperature feedbacks in contemporary climate models, *Nature Geoscience*, *7*(3), 181-184.

Rantanen, M., A. Y. Karpechko, A. Lipponen, K. Nordling, O. Hyvärinen, K. Ruosteenoja, T. Vihma, and A. Laaksonen (2022), The Arctic has warmed nearly four times faster than the globe since 1979, *Communications Earth & Environment*, *3*(1), 168.

Ravishankara, A. R., J. S. Daniel, and R. W. Portmann (2009), Nitrous oxide (N2O): the dominant ozone-depleting substance emitted in the 21st century, *science*, *326*(5949), 123-125.

Rees, R. M., J. Augustin, G. Alberti, B. C. Ball, P. Boeckx, A. Cantarel, S. Castaldi, N. Chirinda, B. Chojnicki, and M. Giebels (2013), Nitrous oxide emissions from European agriculture–an analysis of variability and drivers of emissions from field experiments, *Biogeosciences*, *10*(4), 2671-2682.

Repo, M. E., S. Susiluoto, S. E. Lind, S. Jokinen, V. Elsakov, C. Biasi, T. Virtanen, and P. J. Martikainen (2009), Large N2O emissions from cryoturbated peat soil in tundra, *Nature Geoscience*, *2*(3), 189-192.

Risk, N., D. Snider, and C. Wagner-Riddle (2013), Mechanisms leading to enhanced soil nitrous oxide fluxes induced by freeze–thaw cycles, *Canadian Journal of Soil Science*, *93*(4), 401-414.

Stewart, K. J., M. E. Brummell, R. E. Farrell, and S. D. Siciliano (2012), N2O flux from plant-soil systems in polar deserts switch between sources and sinks under different light conditions, *Soil Biology and Biochemistry*, *48*, 69-77.

Sun, X., X. Han, F. Ping, L. Zhang, K. Zhang, M. Chen, and W. Wu (2018), Effect of rice-straw biochar on nitrous oxide emissions from paddy soils under elevated CO2 and temperature, *Science of the total environment*, *628*, 1009-1016.

Sun, Y., D. S. Goll, J. Chang, P. Ciais, B. Guenet, J. Helfenstein, Y. Huang, R. Lauerwald, F. Maignan, and V. Naipal (2021), Global evaluation of the nutrient-enabled version of the land surface model ORCHIDEE-CNP v1. 2 (r5986), *Geoscientific Model Development*, *14*(4), 1987-2010.

Thompson, R. L., K. Ishijima, E. Saikawa, M. Corazza, U. Karstens, P. K. Patra, P. Bergamaschi, F. Chevallier, E. Dlugokencky, and R. G. Prinn (2014), TransCom N 2 O model inter-comparison–Part 2: Atmospheric inversion estimates of N 2 O emissions, *Atmospheric Chemistry and Physics*, *14*(12), 6177-6194.

Thompson, R. L., L. Lassaletta, P. K. Patra, C. Wilson, K. C. Wells, A. Gressent, E. N. Koffi, M. P. Chipperfield, W. Winiwarter, and E. A. Davidson (2019), Acceleration of global N2O emissions seen from two decades of atmospheric inversion, *Nature Climate Change*, *9*(12), 993-998.

Tian, H., G. Chen, C. Lu, X. Xu, D. J. Hayes, W. Ren, S. Pan, D. N. Huntzinger, and S. C. Wofsy (2015), North American terrestrial CO2 uptake largely offset by CH4 and N2O emissions: toward a full accounting of the greenhouse gas budget, *Climatic change*, *129*(3-4), 413-426.

Tian, H., J. Yang, R. Xu, C. Lu, J. G. Canadell, E. A. Davidson, R. B. Jackson, A. Arneth, J. Chang, and P. Ciais (2019), Global soil nitrous oxide emissions since the preindustrial era estimated by an ensemble of terrestrial biosphere models: Magnitude, attribution, and uncertainty, *Global change biology*, *25*(2), 640-659.

Tian, H., R. Xu, J. G. Canadell, R. L. Thompson, W. Winiwarter, P. Suntharalingam, E. A. Davidson, P. Ciais, R. B. Jackson, and G. Janssens-Maenhout (2020), A comprehensive quantification of global nitrous oxide sources and sinks, *Nature*, *586*(7828), 248-256.

Tian, H., et al. (2018), The Global N2O Model Intercomparison Project, *Bulletin of the American Meteorological Society*, *99*(6), 1231-1251.

Usyskin-Tonne, A., Y. Hadar, U. Yermiyahu, and D. Minz (2020), Elevated CO2 has a significant impact on denitrifying bacterial community in wheat roots, *Soil Biology and Biochemistry*, *142*, 107697.

Virkkala, A. M., J. Aalto, B. M. Rogers, T. Tagesson, C. C. Treat, S. M. Natali, J. D. Watts, S. Potter, A. Lehtonen, and M. Mauritz (2021), Statistical upscaling of ecosystem CO2 fluxes across the terrestrial tundra and boreal domain: Regional patterns and uncertainties, *Global Change Biology*, *27*(17), 4040-4059.

Voigt, C., R. E. Lamprecht, M. E. Marushchak, S. E. Lind, A. Novakovskiy, M. Aurela, P. J. Martikainen, and C. Biasi (2017a), Warming of subarctic tundra increases emissions of all three important greenhouse gases–carbon dioxide, methane, and nitrous oxide, *Global Change Biology*, *23*(8), 3121-3138.

Voigt, C., M. E. Marushchak, R. E. Lamprecht, M. Jackowicz-Korczyński, A. Lindgren, M. Mastepanov, L. Granlund, T. R. Christensen, T. Tahvanainen, and P. J. Martikainen (2017b), Increased nitrous oxide emissions from Arctic peatlands after permafrost thaw, *Proceedings of the National Academy of Sciences*, *114*(24), 6238-6243.

Voigt, C., M. E. Marushchak, B. W. Abbott, C. Biasi, B. Elberling, S. D. Siciliano, O. Sonnentag, K. J. Stewart, Y. Yang, and P. J. Martikainen (2020), Nitrous oxide emissions from permafrost-affected soils, *Nature Reviews Earth & Environment*, *1*(8), 420-434.

Wagner-Riddle, C., K. A. Congreves, D. Abalos, A. A. Berg, S. E. Brown, J. T. Ambadan, X. Gao, and M. Tenuta (2017), Globally important nitrous oxide emissions from croplands induced by freeze–thaw cycles, *Nature Geoscience*, *10*(4), 279-283.

Walker, A. P., M. G. De Kauwe, A. Bastos, S. Belmecheri, K. Georgiou, R. F. Keeling, S. M. McMahon, B. E. Medlyn, D. J. P. Moore, and R. J. Norby (2021), Integrating the evidence for a terrestrial carbon sink caused by increasing atmospheric CO2, *New Phytologist*, *229*(5), 2413-2445.

Wang, X., S. Siciliano, B. Helgason, and A. Bedard-Haughn (2017), Responses of a mountain peatland to increasing temperature: A microcosm study of greenhouse gas emissions and microbial community dynamics, *Soil Biology and Biochemistry*, *110*, 22-33.

Watts, J. D., J. S. Kimball, L. A. Jones, R. Schroeder, and K. C. McDonald (2012), Satellite Microwave remote sensing of contrasting surface water inundation changes within the Arctic–Boreal Region, *Remote Sensing of Environment*, *127*, 223-236.

Wells, K. C., et al. (2018), Top-down constraints on global N2O emissions at optimal resolution: application of a new dimension reduction technique, *Atmos. Chem. Phys.*, *18*(2), 735-756.

Wilson, C., M. P. Chipperfield, M. Gloor, and F. Chevallier (2014), Development of a variational flux inversion system (INVICAT v1. 0) using the TOMCAT chemical transport model, *Geoscientific Model Development*, *7*, 2485-2500.

Yang, G., Y. Peng, M. E. Marushchak, Y. Chen, G. Wang, F. Li, D. Zhang, J. Wang, J. Yu, and L. Liu (2018), Magnitude and pathways of increased nitrous oxide emissions from uplands following permafrost thaw, *Environmental science & technology*, *52*(16), 9162-9169.

You, Y., and S. Pan (2020), Urban Vegetation Slows Down the Spread of Coronavirus Disease (COVID‐19) in the United States, *Geophysical Research Letters*, *47*(18), e2020GL089286.

Zaehle, S., P. Ciais, A. D. Friend, and V. Prieur (2011), Carbon benefits of anthropogenic reactive nitrogen offset by nitrous oxide emissions, *Nature Geoscience*, *4*(9), 601-605.

Soil nitrous oxide emissions across the northern high latitudes

Naiqing Pan[1], Hanqin Tian[1,2*], Hao Shi[3], Shufen Pan[4,1], Josep G. Canadell[5], Jinfeng Chang[6], Philippe Ciais[7], Eric A. Davidson[8], Gustaf Hugelius[9,10], Akihiko Ito[11], Robert B. Jackson[12], Fortunat Joos[13], Sebastian Lienert[13], Dylan B. Millet[14], Stefan Olin[15], Prabir K. Patra[16], Rona L. Thompson[17], Nicolas Vuichard[7], Kelley C. Wells[14], Chris Wilson[18,19], Yongfa You[1], Sönke Zaehle[20]

[1]Center for Earth System Science and Global Sustainability, Schiller Institute for Integrated Science and Society, Boston College, Chestnut Hill, MA, USA

[2]Department of Earth and Environmental Sciences, Boston College, Chestnut Hill, MA, USA

[3]State Key Laboratory of Urban and Regional Ecology, Research Center for Eco-Environmental Sciences, Chinese Academy of Sciences, Beijing, China

[4]Department of Engineering and Environmental Studies Program, Boston College, Chestnut Hill, MA, USA

5Global Carbon Project, CSIRO Oceans and Atmosphere, Canberra, Australian Capital Territory, Australia

[6] College of Environmental and Resource Sciences, Zhejiang University, Hangzhou, China

[7]Laboratoire des Sciences du Climat et de l'Environnement, LSCE, CEA CNRS, UVSQ UPSACLAY, Gif sur Yvette, France

[8]Appalachian Laboratory, University of Maryland Center for Environmental Science, Frostburg, MD, USA

[9]Department of Physical Geography, Stockholm University, Stockholm, Sweden

[10] Bolin Centre for Climate Research, Stockholm University, Stockholm, Sweden

[11] National Institute for Environmental Studies, Tsukuba, Japan

[12] Department of Earth System Science, Woods Institute for the Environment, Precourt Institute for Energy, Stanford University, Stanford, CA, USA

[13] Climate and Environmental Physics, Physics Institute and Oeschger Centre for Climate Change Research, University of Bern, Bern, Switzerland

[14] Department of Soil, Water, and Climate, University of Minnesota, St Paul, MN, USA

[15] Department of Physical Geography and Ecosystem Science, Lund University, Lund, Sweden

[16] Research Institute for Global Change, JAMSTEC, Yokohama, Japan

[17] Norsk Institutt for Luftforskning, NILU, Kjeller, Norway

[18] National Centre for Earth Observation, University of Leeds, Leeds, UK

[19] Institute for Climate and Atmospheric Science, School of Earth & Environment, University of Leeds, Leeds, UK

[20] Max Planck Institute for Biogeochemistry, Jena, Germany

*Corresponding author: Hanqin Tian (hanqin.tian@bc.edu)

Geophysical Research Letters (Submitted on January 18, 2024)

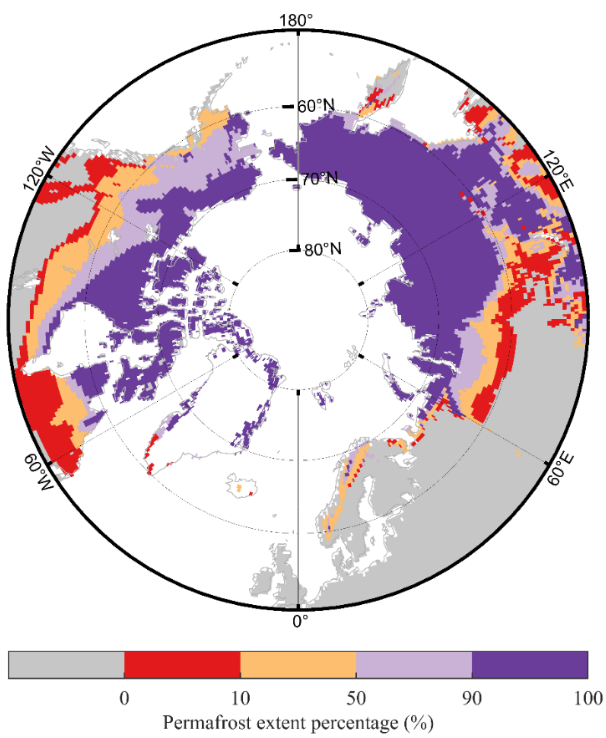

Fig. S1: Spatial distribution of the percentage of permafrost extent in the Northern Hemisphere.

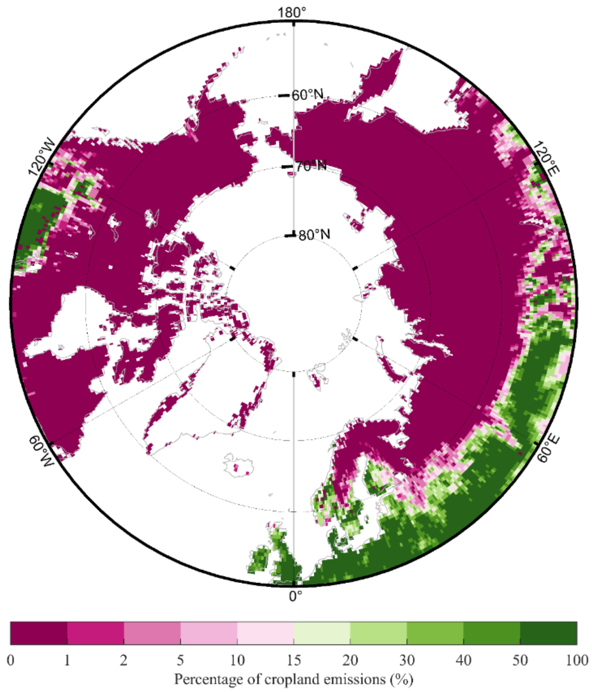

Fig. S2: Spatial distribution of the percentage of soil N_2O emissions from croplands.

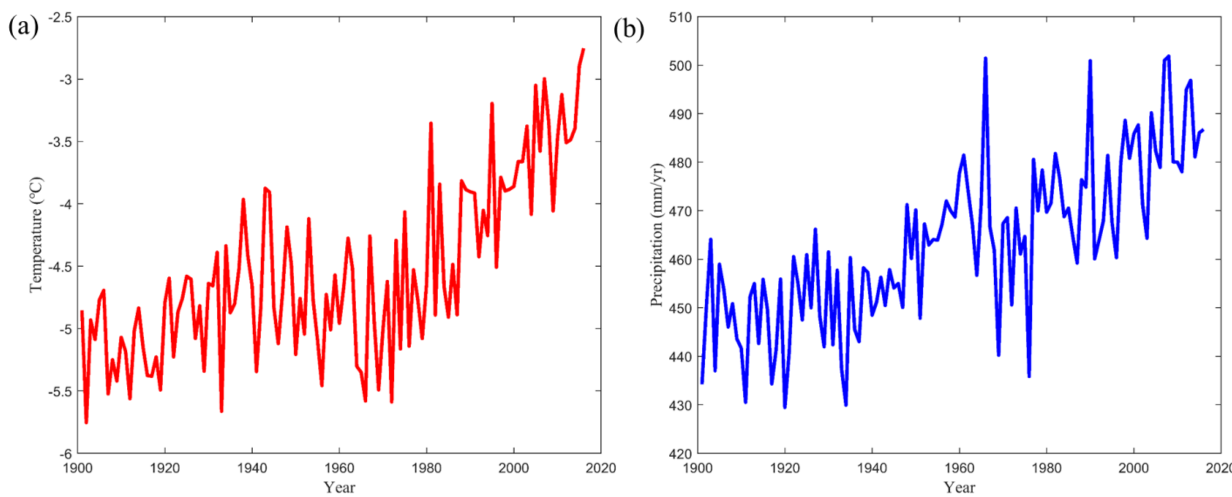

Fig. S3: Temporal variations in mean temperature (a) and precipitation (b) of the northern high latitudes during 1901-2016.

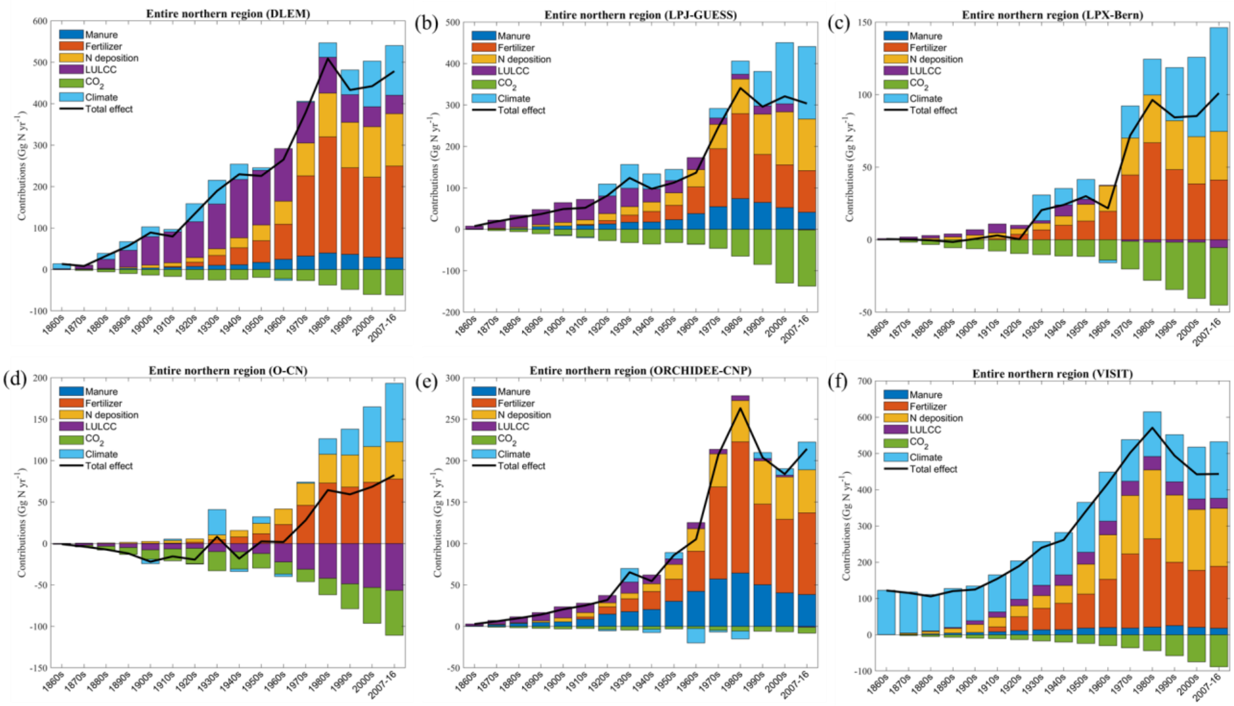

Fig. S4: Decadal variations in the contributions of different driving factors to soil N_2O emissions from the entire northern high latitudes estimated by individual NMIP model.

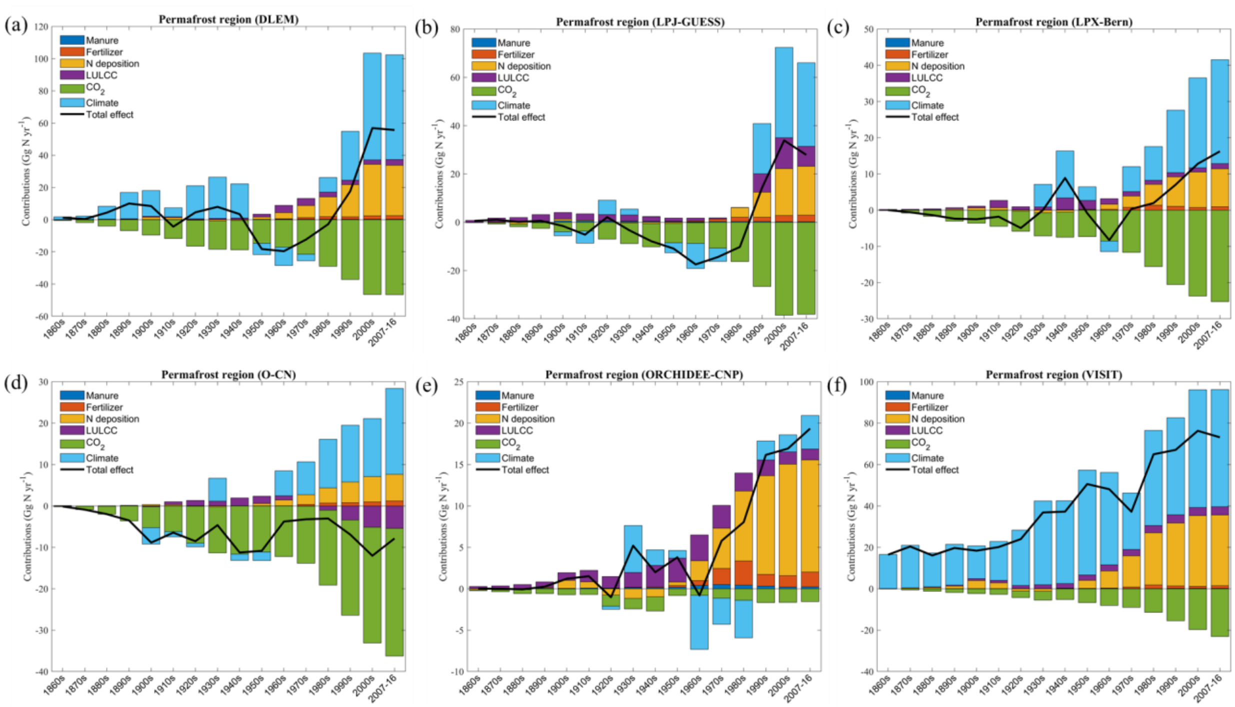

Fig. S5: Decadal variations in the contributions of different driving factors to soil N_2O emissions from permafrost regions estimated by individual NMIP model.

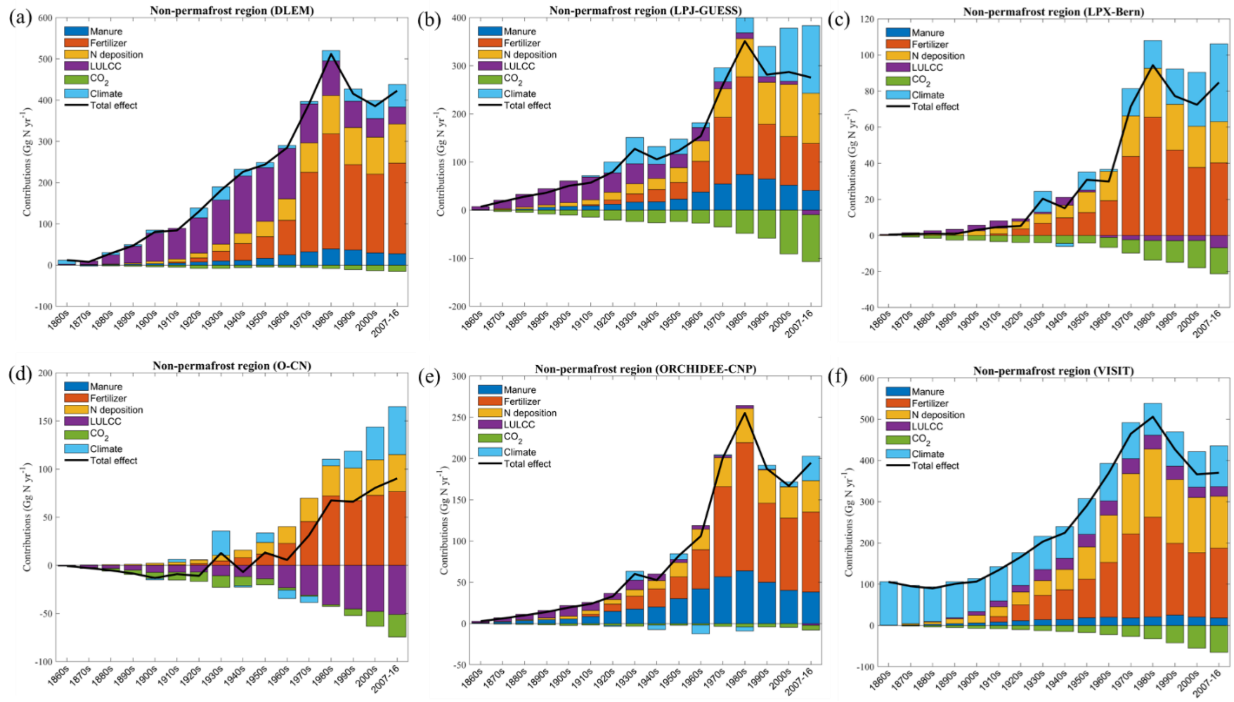

Fig. S6: Decadal variations in the contributions of different driving factors to soil N_2O emissions from non-permafrost regions estimated by individual NMIP model.

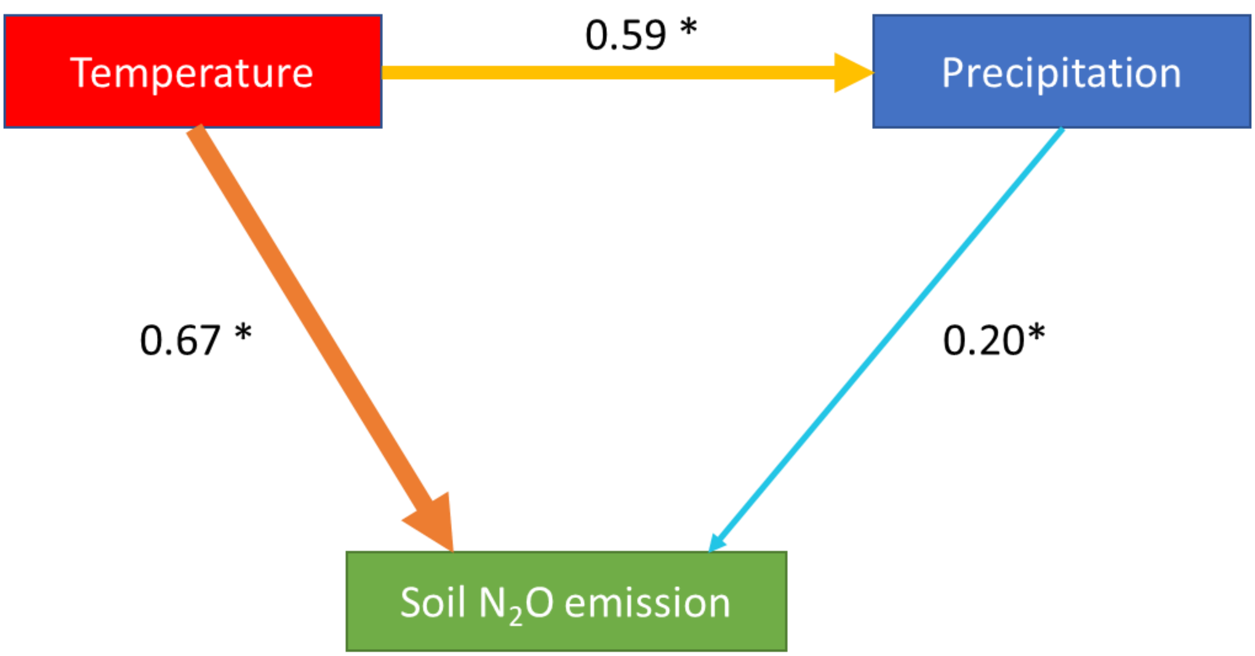

Fig. S7: Path analysis results. Numbers adjacent to arrows in the path diagrams are standardized path coefficients indicating the magnitude of the influence between factors, and the significance level is indicated by * ($p < 0.01$).

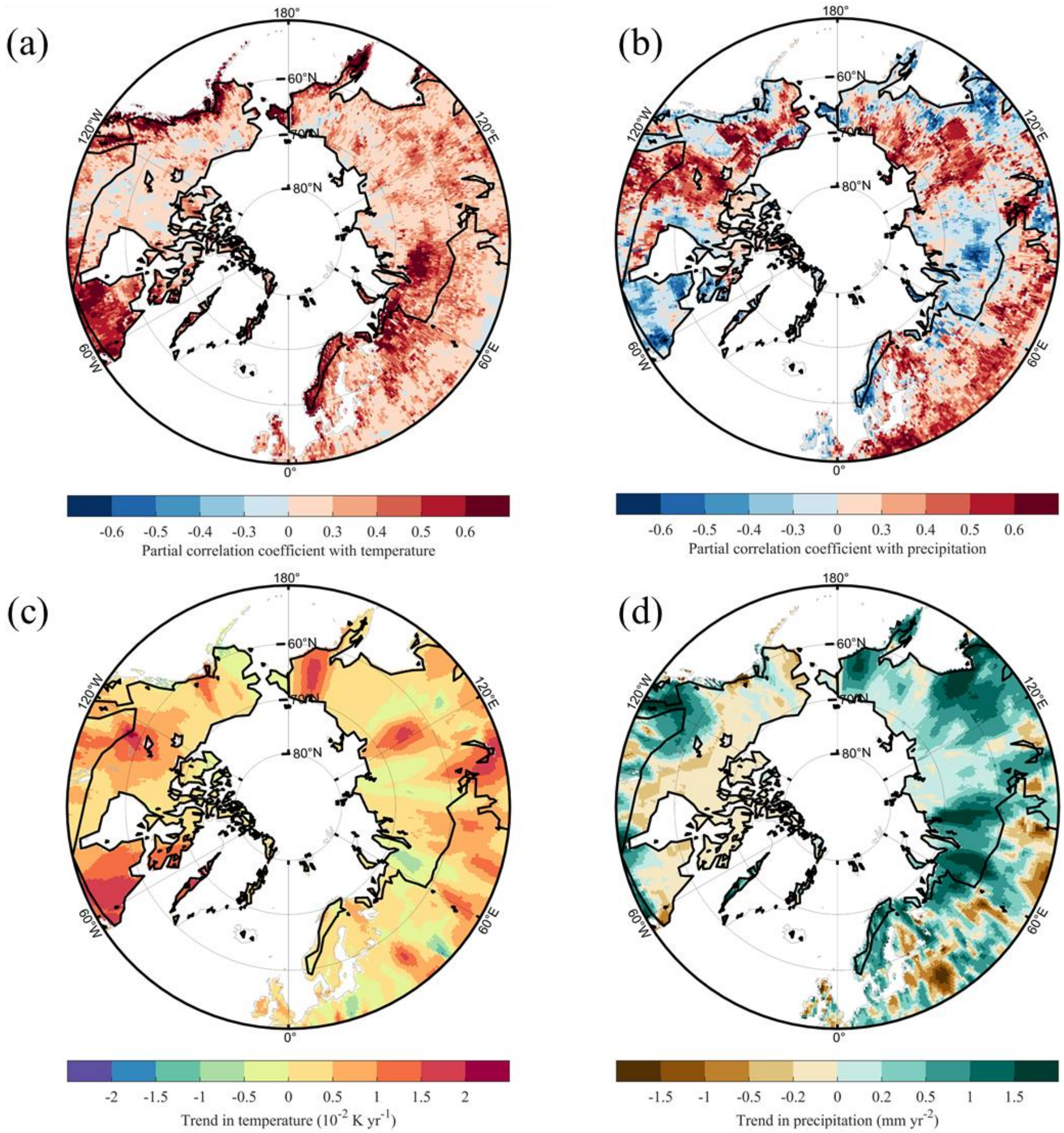

Fig. S8: Spatial distributions of the partial correlation coefficients between modelled annual soil N_2O emissions and temperature (a) and precipitation (b) during 1901-1980; (c) and (d) show trends in temperature and precipitation during 1901-1980, respectively. The black lines in (a)-(d) show the extent of the permafrost region.

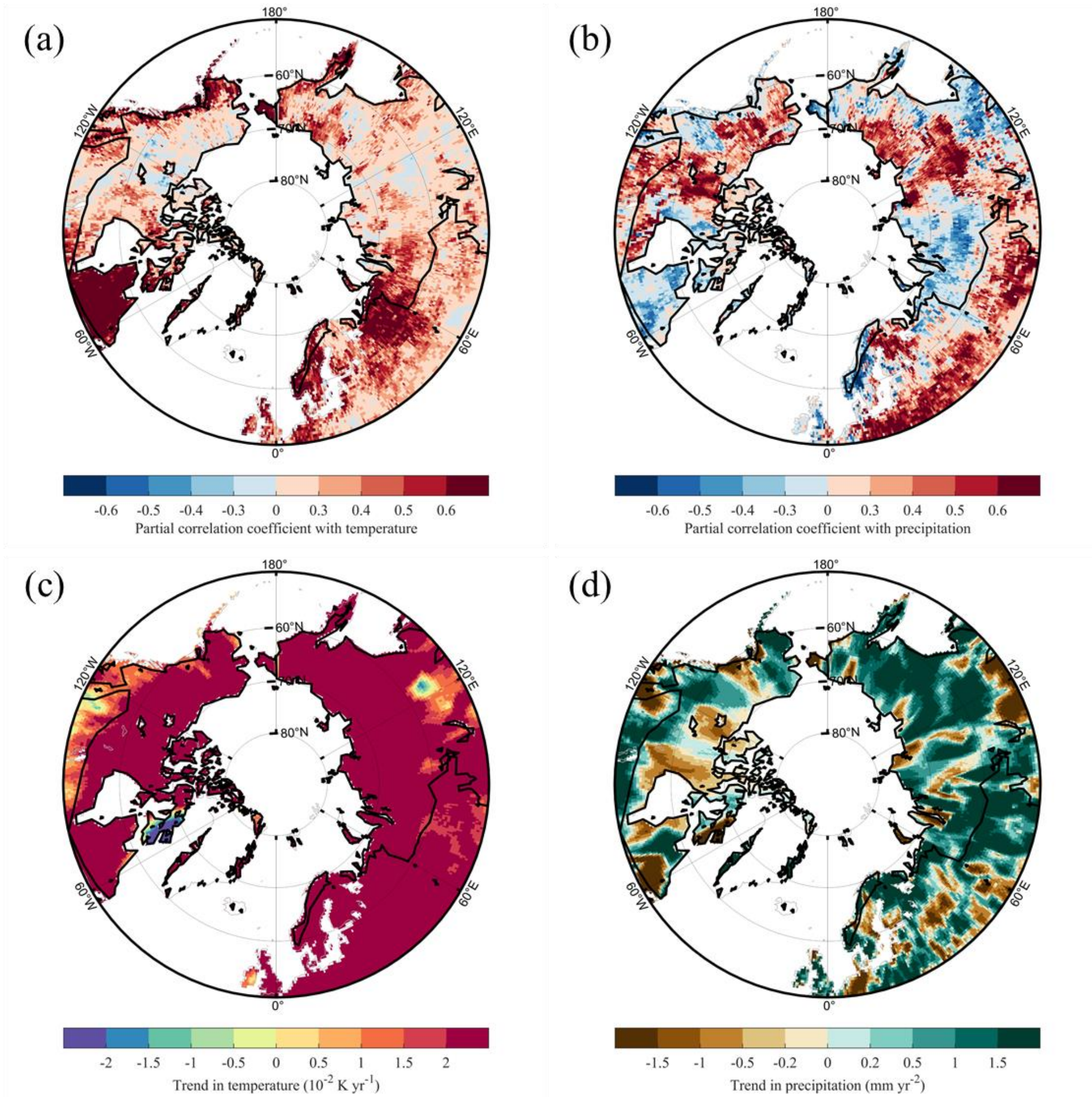

Fig. S9: Spatial distributions of the partial correlation coefficients between modelled annual soil N_2O emissions and temperature (a) and precipitation (b) during 1980-2016; (c) and (d) show trends in temperature and precipitation during 1980-2016, respectively. The black lines in (a)-(d) show the extent of the permafrost region.

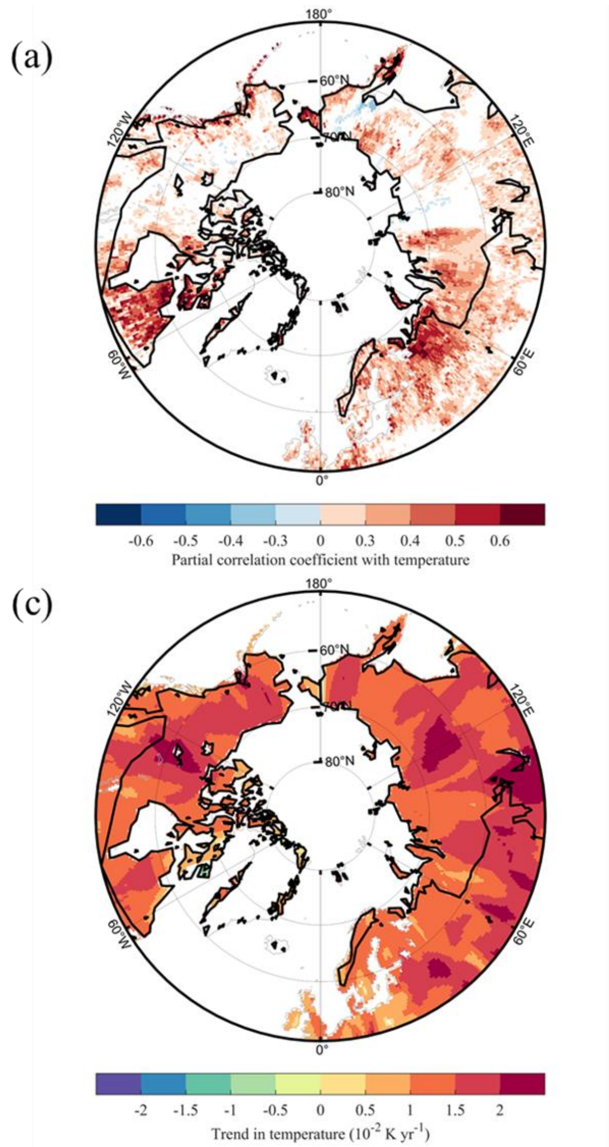

Fig. S10: Trends in temperature and precipitation and their partial correlation coefficients with soil N_2O emissions. a and b show spatial distributions of the partial correlation coefficients for modelled annual soil N_2O emissions versus temperature and precipitation during 1901-2016; grids with non-significant correlation (p>=0.05) were excluded. c and d show trends in temperature and precipitation during 1901-2016, respectively; grids with non-significant trends (*p*>=0.05) were excluded. The black lines in (a)-(d) show the extent of the permafrost region.

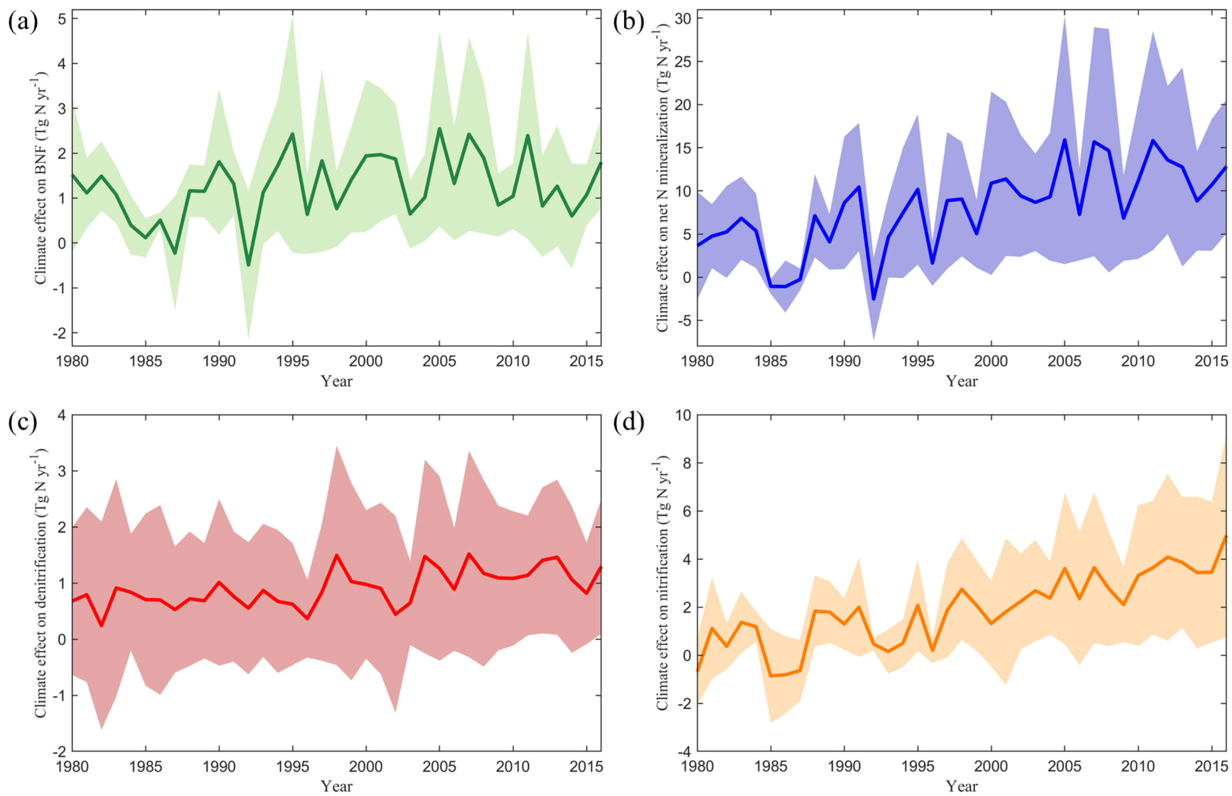

Fig. S11: Climate effects on reactive N flows of the northern high latitudes. (a)-(d) show the effects of climate change on regional biological N fixation, net N mineralization, denitrification, and nitrification, respectively, the lines represent the ensemble means of NMIP model estimates and the shaded areas indicate one standard deviation of model estimates.

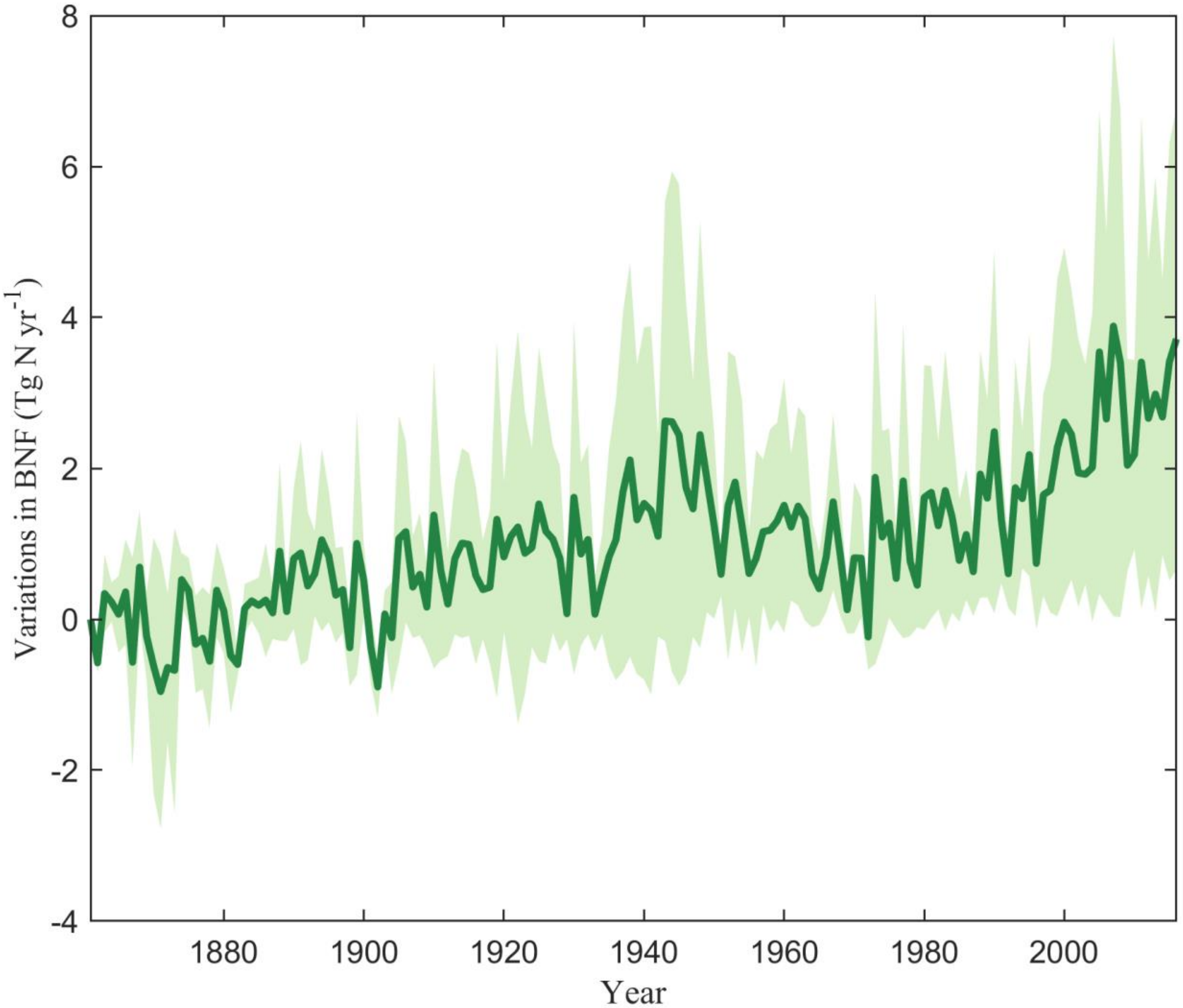

Fig. S12: Temporal variations in the total biological nitrogen fixation in the northern high latitudes during 1861-2016. The line represents the ensemble means of NMIP model estimates and the shaded area indicates one standard deviation of model estimates.

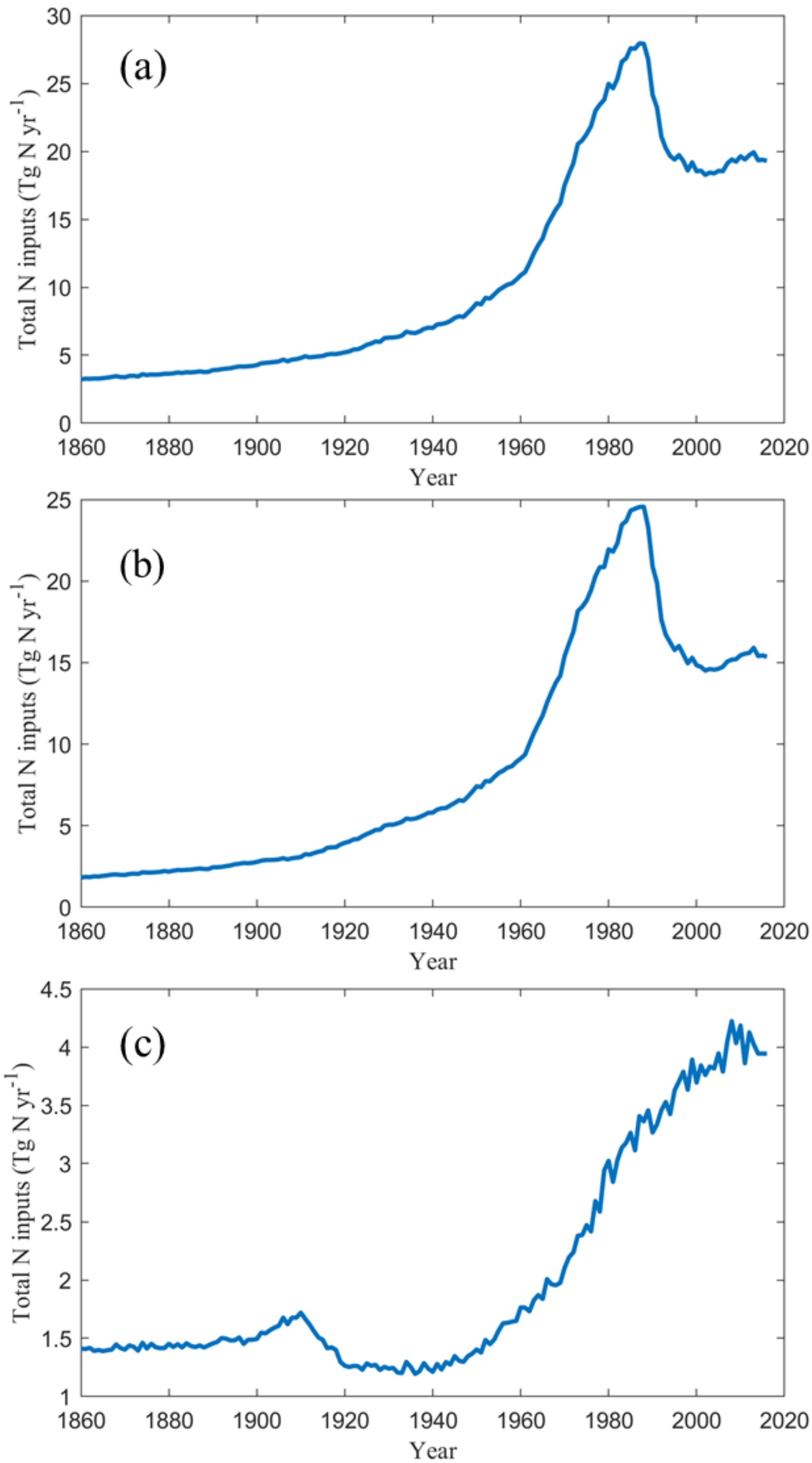

Fig. S13: Temporal variations in the total N inputs in entire northern high latitudes (a), non-permafrost region (b) and permafrost region (c).

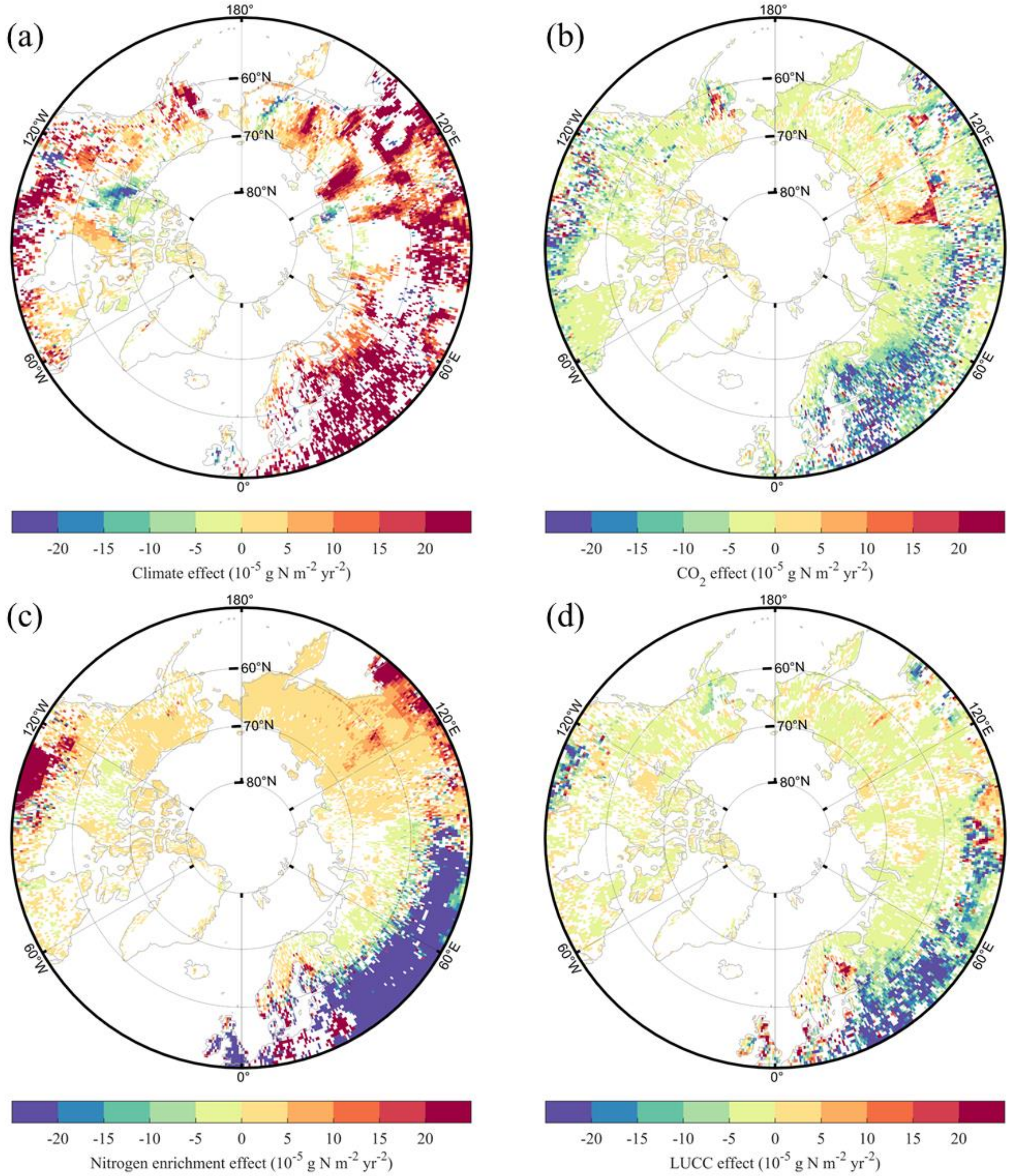

Fig. S14: Spatial patterns of the effects of different driving factors during the period 1980-2016. (a)-(d) show the effects of climate, CO_2, nitrogen enrichment and LULCC, respectively. Grids with non-significant trends (p>=0.05) were excluded.

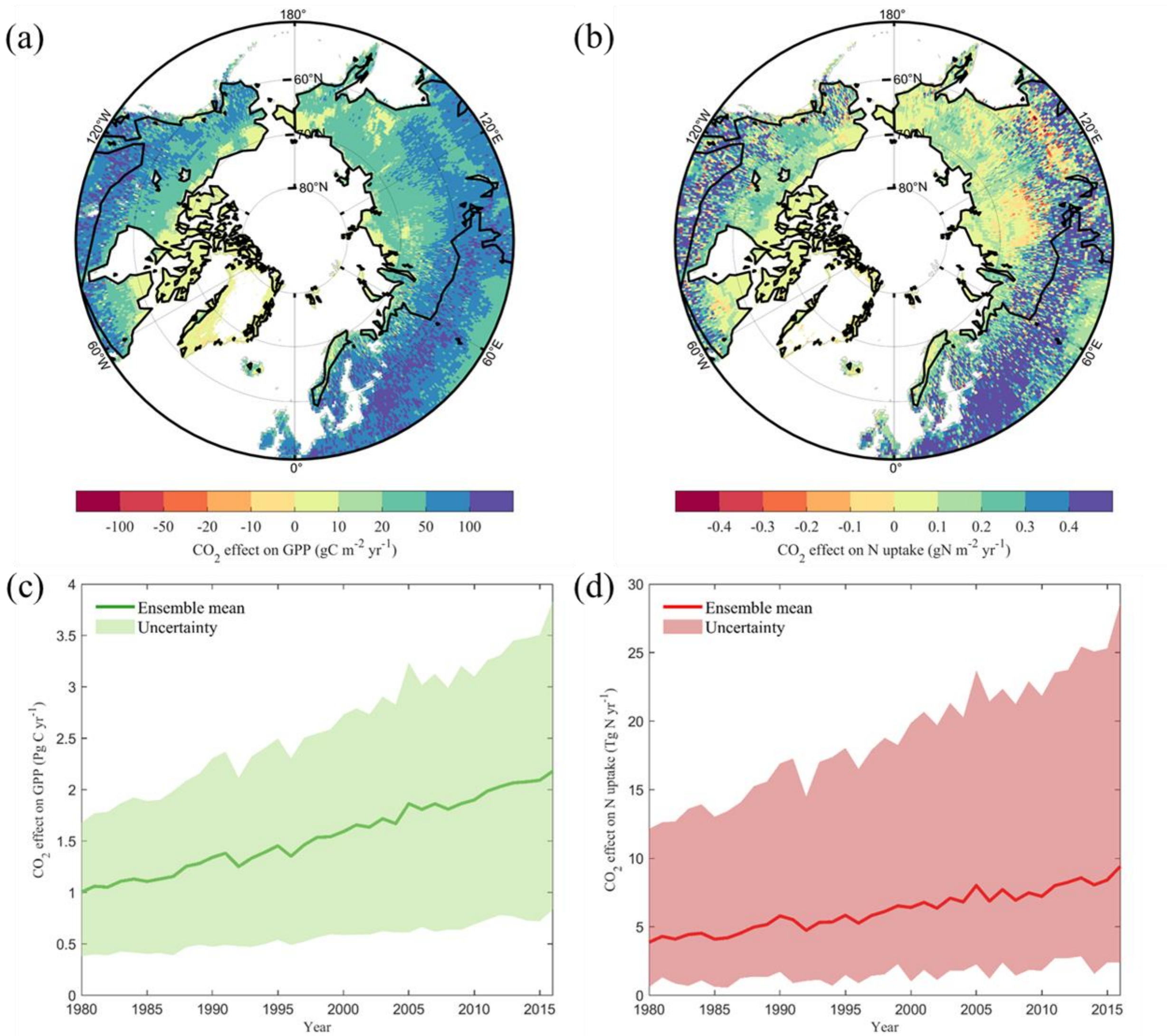

Fig. S15: The effects of increasing CO_2 concentration on ecosystem GPP and plant nitrogen uptake. (a) and (b) show spatial distributions of modelled average CO_2 effects on GPP and nitrogen uptake during 1980-2016, respectively; black lines show the extent of the permafrost region. (c) and (d) show the temporal variations in CO_2 effects on regional GPP and nitrogen uptake, respectively; the lines represent the ensemble means of all NMIP model estimates and the shaded areas show minimum and maximum estimates.

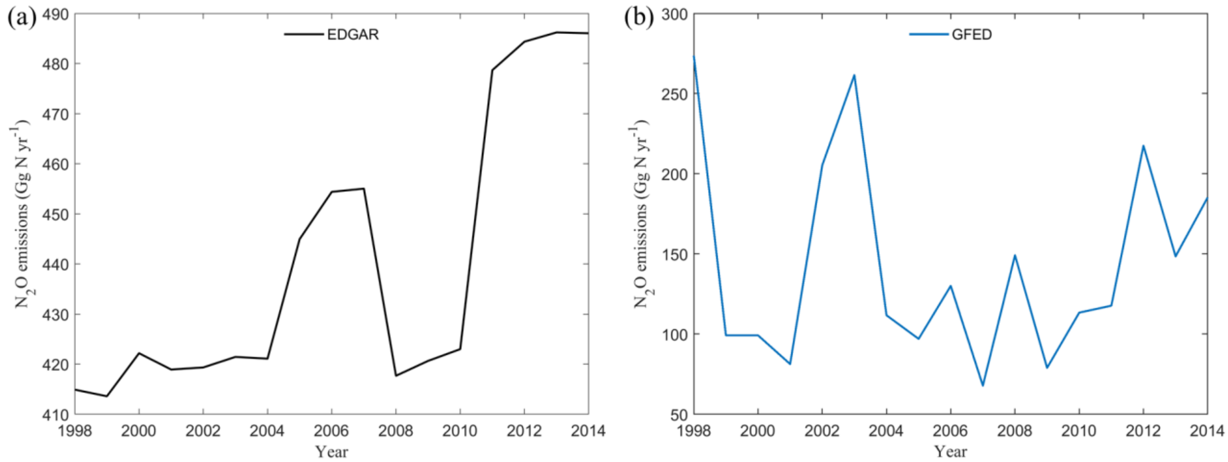

Fig. S16: Interannual variations in N_2O emissions from non-soil anthropogenic sources (a) and biomass burning (b).

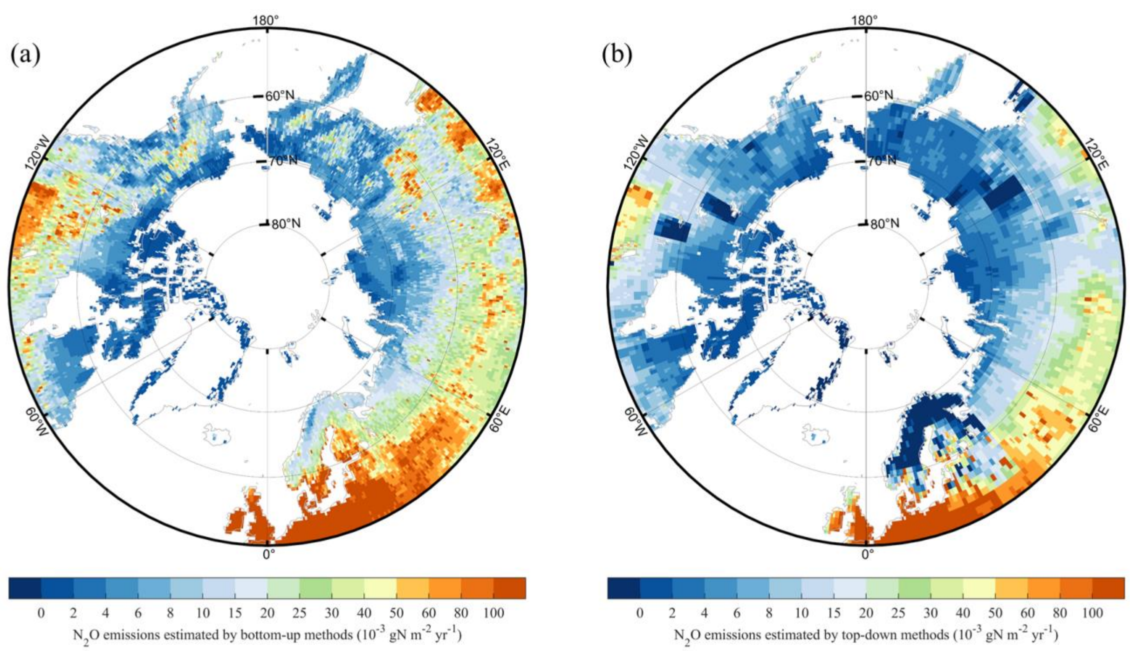

Fig. S17. Uncertainty in soil N_2O emissions estimated by NMIP models (a) and in total N_2O emissions estimated by top-down models (b). Here, one standard deviation of all model estimates was used to indicate uncertainty.

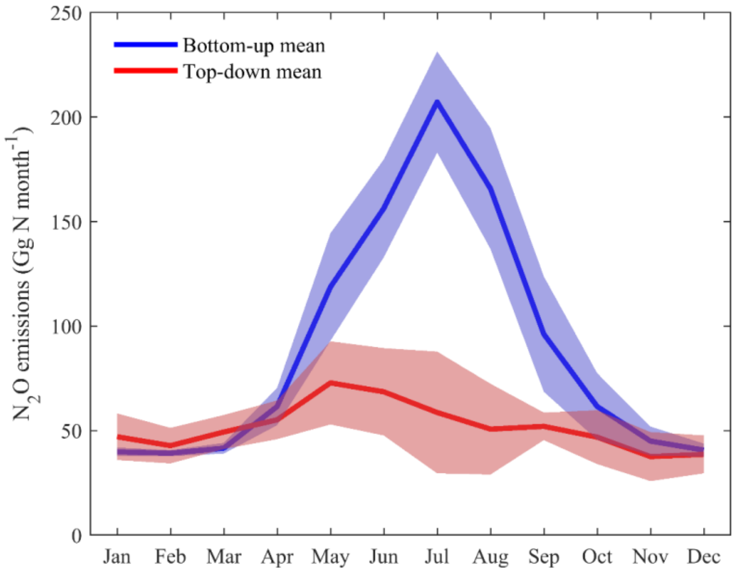

Fig. S18. Comparison of intra-annual fluctuations of N_2O emissions estimated by TD and BU approaches.

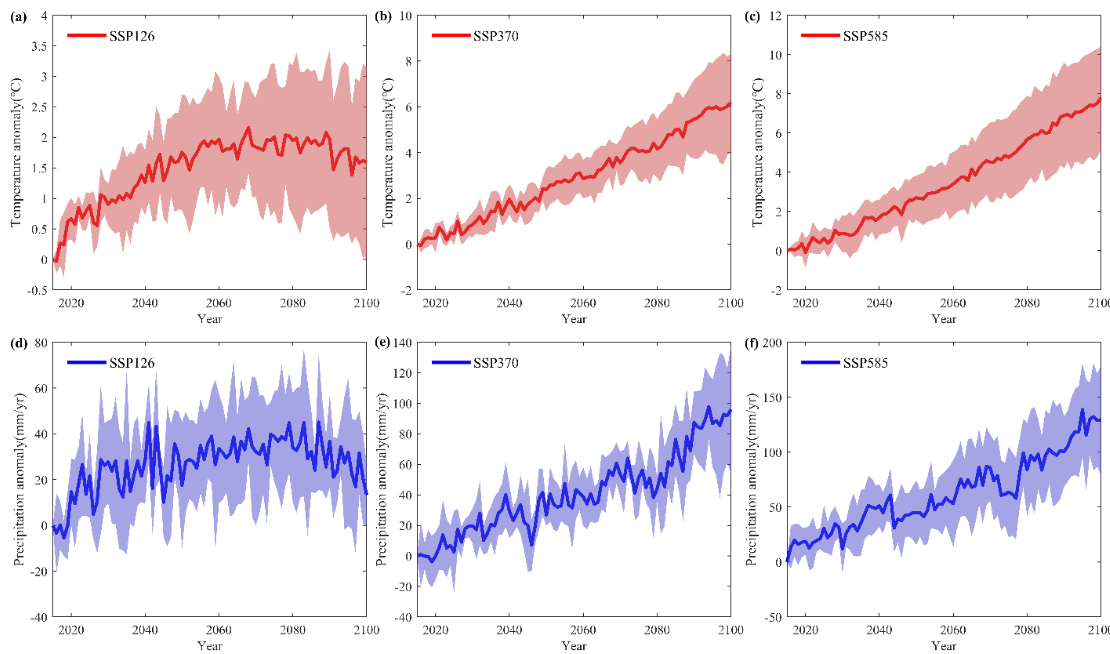

Fig. S19: Future variations in temperature and precipitation of the northern high latitudes under different SSP scenarios. Future temperature and precipitation data were from Inter-Sectoral Impact Model Intercomparison Project (ISIMIP) phase 3b, which were supplied based on Climate Model Intercomparison Project Phase 6 (CMIP6) output of five climate models: GFDL-ESM4, IPSL-CM6A-LR, MPI-ESM1-2-HR, MRI-ESM2-0 and UKESM1-0-LL.

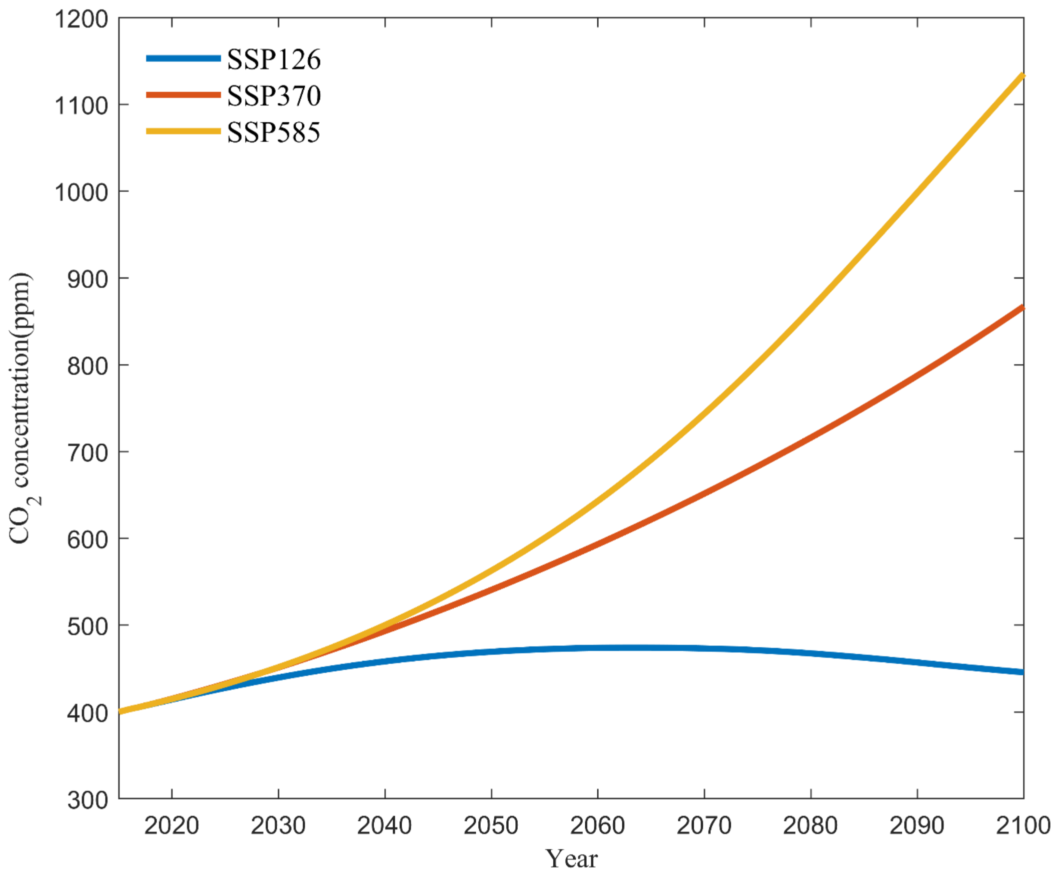

Fig. S20: Future variations in atmospheric CO_2 concentration under different SSP scenarios.

Table S1: Model simulation design

Historical	Climate	CO_2	LULCC	N deposition	N fertilizer	Manure N
S0	1901-1920	1860	1860	1860	1860	1860
S1	•	•	•	•	•	•
S2	•	•	•	•	•	1860
S3	•	•	•	•	1860	1860
S4	•	•	•	1860	1860	1860
S5	•	•	1860	1860	1860	1860
S6	•	1860	1860	1860	1860	1860

Note: "•" indicates the forcing during 1860-2016 is included in the simulation, "1901-1920" indicates the 20-year mean climate condition during 1901-1920 was used over the entire simulation period, and "1860" indicates the forcing was fixed in 1860 level over the entire period. Climate data was only available from 1901, we used the 20-yr average value between 1901 and 1920 for years 1860-1900.

Table S2: Spatial and temporal resolution of bottom-up and top-down models used in this study.

Bottom-up estimates				
Name	Sector	Spatial resolution	Temporal coverage	References
DLEM	Soil	0.5°×0.5°	1860-2016	Tian et al. (2015)
LPJ-GUESS	Soil	0.5°×0.5°	1860-2016	Olin et al. (2015)
LPX-Bern	Soil	0.5°×0.5°	1860-2016	Stocker et al. (2013)
O-CN	Soil	1°×1°	1860-2016	Zaehle et al. (2011)
ORCHIDEE-CNP	Soil	2°×2°	1860-2016	Goll et al. (2017)
VISIT	Soil	0.5°×0.5°	1860-2016	Inatomi et al. (2010)
EDGARv6.0	Multiple sources (see method)	0.1°×0.1°	1970-2018	Crippa et al. (2019)
GFED4.1s	Biomass burning	0.25°×0.25°	1997-2021	Van Der Werf et al. (2017)
Top-down estimates				
Name (ACTM)	Resolution of state vector	ACTM horizontal resolution	Temporal coverage	References
GEOSChem	5°×4°	5°×4°	1998-2016	Wells et al. (2018)
INVICAT	5.625°×5.625°	5.625°×5.625°	1998-2014	Wilson et al. (2014)
MIROC4-ACTM	84 regions	2.8°×2.8°	1998-2016	Patra et al. (2018)

References

Crippa, M., Oreggioni, G., Guizzardi, D., Muntean, M., Schaaf, E., Lo Vullo, E., Solazzo, E., Monforti-Ferrario, F., Olivier, J. G. J., & Vignati, E. (2019). Fossil CO2 and GHG emissions of all world countries. *Publication Office of the European Union: Luxemburg*.

Goll, D. S., Vuichard, N., Maignan, F., Jornet-Puig, A., Sardans, J., Violette, A., Peng, S., Sun, Y., Kvakic, M., Guimberteau, M., Guenet, B., Zaehle, S., Penuelas, J., Janssens, I., & Ciais, P. (2017). A representation of the phosphorus cycle for ORCHIDEE (revision 4520). *Geosci. Model Dev.*, *10*(10), 3745-3770. https://doi.org/10.5194/gmd-10-3745-2017

Inatomi, M., Ito, A., Ishijima, K., & Murayama, S. (2010). Greenhouse gas budget of a cool-temperate deciduous broad-leaved forest in Japan estimated using a process-based model. *Ecosystems*, *13*(3), 472-483.

Olin, S., Lindeskog, M., Pugh, T. A. M., Schurgers, G., Wårlind, D., Mishurov, M., Zaehle, S., Stocker, B. D., Smith, B., & Arneth, A. (2015). Soil carbon management in large-scale Earth system modelling: implications for crop yields and nitrogen leaching. *Earth System Dynamics*, *6*(2), 745-768.

Patra, P. K., Takigawa, M., Watanabe, S., Chandra, N., Ishijima, K., & Yamashita, Y. (2018). Improved chemical tracer simulation by MIROC4. 0-based atmospheric chemistry-transport model (MIROC4-ACTM). *Sola*, *14*, 91-96.

Stocker, B. D., Roth, R., Joos, F., Spahni, R., Steinacher, M., Zaehle, S., Bouwman, L., & Prentice, I. C. (2013). Multiple greenhouse-gas feedbacks from the land biosphere under future climate change scenarios. *Nature Climate Change*, *3*(7), 666-672.

Tian, H., Chen, G., Lu, C., Xu, X., Ren, W., Zhang, B., Banger, K., Tao, B., Pan, S., & Liu, M. (2015). Global methane and nitrous oxide emissions from terrestrial ecosystems due to multiple environmental changes. *Ecosystem Health and Sustainability*, *1*(1), 1-20.

Van Der Werf, G. R., Randerson, J. T., Giglio, L., Van Leeuwen, T. T., Chen, Y., Rogers, B. M., Mu, M., Van Marle, M. J. E., Morton, D. C., & Collatz, G. J. (2017). Global fire emissions estimates during 1997-2016.

Wells, K. C., Millet, D. B., Bousserez, N., Henze, D. K., Griffis, T. J., Chaliyakunnel, S., Dlugokencky, E. J., Saikawa, E., Xiang, G., Prinn, R. G., O'Doherty, S., Young, D., Weiss, R. F., Dutton, G. S., Elkins, J. W., Krummel, P. B., Langenfelds, R., & Steele, L. P. (2018). Top-down constraints on global N2O emissions at optimal resolution: application of a new dimension reduction technique. *Atmos. Chem. Phys.*, *18*(2), 735-756. https://doi.org/10.5194/acp-18-735-2018

Wilson, C., Chipperfield, M. P., Gloor, M., & Chevallier, F. (2014). Development of a variational flux inversion system (INVICAT v1. 0) using the TOMCAT chemical transport model. *Geoscientific Model Development*, *7*, 2485-2500.

Zaehle, S., Ciais, P., Friend, A. D., & Prieur, V. (2011). Carbon benefits of anthropogenic reactive nitrogen offset by nitrous oxide emissions. *Nature Geoscience*, *4*(9), 601-605.